August 2018

Conformal Mapping Improvement of the Boundary Element Method Solution for Underground Water Flow in a Domain with a Very Singular Boundary

Megan Romero
meganromero325@gmail.com

CONFORMAL MAPPING IMPROVEMENT OF THE BOUNDARY ELEMENT METHOD SOLUTION FOR UNDERGROUND WATER FLOW IN A DOMAIN WITH A VERY SINGULAR BOUNDARY

By

Megan Romero

Bachelor of Science - Mathematics
University of Nevada, Las Vegas
2013

A thesis submitted in partial fulfillment
of the requirements for the

Master of Science - Mathematical Sciences

Department of Mathematical Sciences
College of Sciences
The Graduate College

University of Nevada, Las Vegas
August 2018

UNLV | GRADUATE COLLEGE

Thesis Approval

The Graduate College
The University of Nevada, Las Vegas

July 27, 2018

This thesis prepared by

Megan Romero

entitled

Conformal Mapping Improvement of the Boundary Element Method Solution for Underground Water Flow in a Domain with a Very Singular Boundary

is approved in partial fulfillment of the requirements for the degree of

Master of Science - Mathematical Sciences
Department of Mathematical Sciences

Angel Muleshkov, Ph.D.
Examination Committee Chair

Kathryn Hausbeck Korgan, Ph.D.
Graduate College Interim Dean

Zhonghai Ding, Ph.D.
Examination Committee Member

Michelle Robinette, Ph.D.
Examination Committee Member

Stephen Lepp, Ph.D.
Graduate College Faculty Representative

Abstract

Conformal Mapping Improvement of the Boundary Element Method Solution for Underground Water Flow in a Domain with a Very Singular Boundary

By

Megan Romero

Dr. Angel Muleshkov, Examination Committee Chair

Associate Professor of Mathematics

University of Nevada, Las Vegas

Numerical solutions using a Boundary Element Method (BEM) for a confined flow in a very singular finite domain are developed. Typically, in scientific journal publications, authors avoid domains with many and more malignant singularities due to the extremely big and difficult to estimate errors in the numerical calculations. Using exact Conformal Mapping solutions for simplified domains with the same singularity as in the original domain, this problem can be solved numerically with improvements introduced by Conformal Mapping solutions. Firstly, to experiment with improving the BEM solution by Conformal Mapping, a domain inside a rectangle is considered. The exact solution inside a rectangle is found by Conformal Mapping. Then solution is obtained from BEM. The singularities in number and malignancy will lead to failure of the Boundary Element solution near the singular points and even much further from them. Then, the BEM solution is improved by Conformal Mapping. For every singularity, the domain will be extended in an easy enough shape, which allows for using Conformal Mapping method to find the exact solution near the singularity for the extended domain. The function that describes the behavior of the solution close to the singularity is imposed to the elements that are adjacent to the corresponding singularities in the BEM calculations, e.g. using $A(x-x_s)^{2/3}$ found by Conformal Mapping instead of $B(x-x_s)$ which leads to the BEM

solution improved by Conformal Mapping. The different methods for finding the solution of the problem inside a rectangle are compared to show the need for improvement of the BEM solution. Then, a more complicated realistic finite domain for which it is impossible to find the exact solution is considered. The problem is solved by BEM and by improving BEM by Conformal Mapping as described above. The calculations are expressed in the form of tables and figures. Additional analysis of the effect of the singularities is given in the conclusions.

Acknowledgments

I would like to thank Dr. Ding, Dr. Lepp, and Dr. Robinette for being on my committee and taking their time to read and review my thesis. I would like to thank Dr. Ding and Dr. Robinette for the knowledge I received from them while taking their classes.

I would especially like to thank Dr. Muleshkov and his wife, Sonya Muleshkov. I have been taking classes with Dr. Muleshkov since 2010, and I have learned so much from him. He has changed the way that I think about and approach mathematics. Dr. Muleshkov and Sonya have been so caring over the years. Sonya was always willing to schedule a time for me to come see Dr. Muleshkov when I requested to meet with him, and provided excellent hospitality. I am truly grateful for them.

I would also like to thank my classmates, Tan Nguyen, Jorge Reyes, and Adam Parks, without whose collaboration during our classes and support while working on my thesis, this thesis would have been impossible.

I would like to thank my church family, colleagues, friends and family for their support and encouragement–particularly, my parents, who have always supported my education and allowed me the time and space to focus on accomplishing my goals. I am blessed by all of you.

Lastly, I would like to thank my husband. During our courtship, engagement, and marriage, I have been progressing toward earning my master's degree. He has been supportive in many different ways, including taking on extra responsibilities around the home to enable me to finish. Not only has he been a source of encouragement to me with school, but he encourages me daily to "run with endurance the race that is set out for us, looking to Jesus, the pioneer and perfect of faith, who for the joy that was set before him endured the cross, despising the shame, and is seated at the right hand of the throne of God" (Heb. 12:2-3, ESV).

Soli Deo Gloria.

Dedication

I wish to dedicate this thesis to my husband, Ed Romero. Thank you for blessing me and loving me, I love you. I wish also to dedicate this to my parents and friends who supported me. In addition, I wish to dedicate this to Dr. Muleshkov and Sonya Muleshkov for all they've taught me and without whom this would have been impossible.

Table of Contents

List of Figures

Chapter 1. Introduction

1.1 Underground Water Flow Modeled by Darcy's Law

Darcy's Law, discovered by experimentation, states that under conditions given below, the discharge velocity of a flow through porous media is linearly dependent on the hydraulic gradient (Harr, 1990; Polubarinova-Kochina, 1962). The conditions to use Darcy's Law to describe a flow through porous media are that the flow must be laminar and the fluid must be viscous (Harr, 1990; Polubarinova-Kochina, 1962). Darcy's Law is used to describe underground water flow because water is a viscous fluid and when it flows through porous media underground, the flow is laminar (Harr, 1990; Polubarinova-Kochina, 1962).

Under the following conditions for underground water flow, Darcy's Law is described by the two-dimensional Laplace PDE. The conditions are: the soil is consistent and its pores are filled with fluid, the fluid is incompressible, and the flow is laminar and has the same movement in parallel planes (Cedergren, 1967; Harr, 1990; Polubarinova-Kochina, 1962). The mathematics of how to obtain the two-dimensional Laplace PDE from Darcy's Law to model underground water flow is given next in this section.

Darcy's Law uses Bernoulli's Equation which states that the total hydraulic head of the flow at any point in a domain is a constant (Harr, 1990; Polubarinova-Kochina, 1962). The constant is determined by the sum of the pressure head, elevation head, and velocity head,

$$H = \frac{p}{\rho g} + z + \frac{v^2}{2g} \tag{1}$$

where H is the total hydraulic head; $\frac{p}{\rho g}$ is the pressure head comprised of p, the atmospheric pressure and ρ, the density of the fluid; z is the elevation head; $\frac{v^2}{2g}$ is the velocity head comprised of v, the velocity and g, gravity (Harr, 1990; Polubarinova-Kochina, 1962). Eq. 2 gives the potential, ϕ,

$$H = \frac{\phi}{g} \tag{2}$$

(Lecture 6).

Since underground water flow moves through the porous media very slowly, $v << 1$, v is negligible. Thus, Eq 1 becomes

$$H = \frac{p}{\rho g} + z \tag{3}$$

Darcy's Law is written as,

$$\vec{v} = -k\nabla H \tag{4}$$

where $\vec{v}$ is the discharge velocity vector, k is the coefficient of permeability which encompasses the permeability of the porous media as well as the density and viscosity of the fluid (Harr, 1990; Polubarinova-Kochina, 1962), and ∇H is the hydraulic gradient.

Since the soil remains consistent and the fluid is incompressible, the Law of Conservation of Mass can by applied to Eq. 4 (Harr, 1990),

$$\text{div}(k\nabla H) = 0 \Longrightarrow \Delta H = 0 \tag{5}$$

thus, one gets the two-dimensional Laplace PDE

$$\frac{\partial^2 H}{\partial x^2} + \frac{\partial^2 H}{\partial y^2} = 0 \tag{6}$$

From Eq. 2 and Eq. 6, one derives that the potential, ϕ, also satisfies the two-dimensional Laplace Equation

$$\frac{\partial^2 \phi}{\partial x^2} + \frac{\partial^2 \phi}{\partial y^2} = 0 \tag{7}$$

In other words, both H and ϕ are harmonic functions.

Thus, underground water flow can be modeled by the two-dimensional Laplace PDE obtained from Darcy's Law.

1.2 Methods of Solving BVPs for the Two-Dimensional Laplace PDE

There are many ways to solve Boundary Value Problems (BVPs) for the two-dimensional Laplace PDE in a domain, D, when given Dirichlet, Neumann, or Robin boundary conditions. This section limits the ways to solve BVPs for the two-dimensional Laplace PDE to only those that are relevant to the types of domains with boundary conditions in this thesis. In this thesis, boundary conditions are either constant Dirichlet or zero Neumann given on each portion of the boundary.

The solution of BVPs for the two-dimensional Laplace PDE inside D can be solved by Conformal Mapping when the boundaries of the domains are generalized polygons with constant Dirichlet or zero Neumann boundary conditions given on each portion of the boundary. A generalized polygon with n vertices in the $z$plane (Riemann Sphere) is either a straight line ($n = 1$) or a union of a finite number ($n > 1$) of line segments or rays, as every end point of a segment is the initial point of the next segment (Muleshkov, 2016). Two segments can not intersect at a point which is interior for both of them. The interior angles, $\pi\alpha_k$, where k goes from 1 to n are connected with the equation $\sum_{k=1}^{n} \alpha_k = n - 2$ (Muleshkov, 2016). The conformal mapping, $f(z) = u(x, y) + iv(x, y)$, solves BVPs for the two-dimensional Laplace PDE inside a generalized polygon. The function, $f(z)$ that maps D onto its image, D^*, is one to one, analytic at every point in D, $f'(z_0) \neq 0$ for every point z_o in D, and preserves the local angles of every point in D (Muleshkov, 2016). The original Riemann Mapping Theorem implies that for every two domains, one domain, D with boundary Γ, in the $x - y$ plane where $z = x + iy$ that is not the entire $x - y$ plane or the empty set and the other domain, D^* with boundary Γ^*, in $u - v$ plane where $w = u + iv$ that is not the whole $u - v$ plane or the empty set, then there exists an analytic function, $w = f(z)$, that maps D onto D^* and the boundary Γ is mapped onto Γ^* as the mapping from D onto D^* is a conformal mapping (Muleshkov, 2016). This mapping is not unique, but if three points, z_1, z_2, and z_3, on Γ correspond to three points w_1, w_2, and w_3, on Γ^* then the mapping is unique (Muleshkov, 2016). Although the Riemann Mapping Theorem gives the existence of a unique conformal mapping of D onto D^*, it does not give how to find the conformal mapping (Carrier, Krook, & Pearson, 2005). The details of how we find the conformal mapping of D onto D^* where Γ and Γ^*

are generalized polygons are given in Chapter 2.1.

There are various numerical methods that can be used to solve BVPs for the two-dimensional Laplace PDE inside a domain enclosed by boundary Γ with constant Dirichlet or zero Neumann boundary conditions given on each portion of the boundary e.g. Boundary Element Method (BEM), Finite Element Method (FEM), various meshless methods, mixed methods, etc. This thesis will concentrate on BEM which is very close to the nature of the given boundary conditions.

BEM is a numerical method based on Green's Second Identity that can be used to solve BVPs for two-dimensional fluid flow problems that are described by the Laplace PDE. On every segment either $\phi = \text{const.}$ is given or the normal derivative, $\frac{\partial \phi}{\partial n} = 0$ is given. When ϕ is equal to a constant, $\frac{\partial \phi}{\partial n}$ is unknown and is approximated by a function found by interpolation between nodes. When $\frac{\partial \phi}{\partial n} = 0$, ϕ is unknown and is approximated by a function that is found by interpolation between nodes. Then, using BEM, the missing values of either ϕ or $\frac{\partial \phi}{\partial n}$ are found at the chosen nodes. Once ϕ and $\frac{\partial \phi}{\partial n}$ have been found at the chosen nodes, then the value of ϕ at an arbitrary point p, denoted by ϕ_p, can be evaluated.

1.3 Overview of Previous Work to find the BEM Solution When There are Singularities on the Boundary of the Domain

There are several articles, papers, and resources available for solving BVPs for the the two-dimensional Laplace PDE using BEM. This overview includes previous work relevant to this thesis, specifically, how others have handled singularities on the boundary when using BEM.

When using BEM, the boundary is discretized into elements, which are small portions of the boundary, with nodes connecting each element. On elements where ϕ is given, $\frac{\partial \phi}{\partial n}$ is approximated by a linear function found by linear interpolation between two nodes where the values of the normal derivative at the nodes are unknown and sought. On elements where $\frac{\partial \phi}{\partial n}$ is given, ϕ is approximated by a linear function found by linear interpolation between two nodes where the values of ϕ at the nodes are unknown and sought. However,

when there are singularities, some books use quadratic, cubic, etc. interpolations on the elements adjacent to the singularities (Kythe, 1995). But, those interpolations are simply a guess - they don't come from the exact solution.

Besides the choice of interpolation, other numerical methods have been developed to handle the singular points on the boundary of the domain. Since $\frac{\partial \phi}{\partial n}$ doesn't exist at corners, there is no node at a corner to represent the value of $\frac{\partial \phi}{\partial n}$. Instead, the node at the corner is eliminated and replaced by a pair of nodes, one on each side of the corner, at a distance of ϵ and δ away from the corner (Bruch, 1991; Kythe, 1995). This method is used in this thesis when finding the BEM solution around boundary points where the normal derivative doesn't exist.

Another method is to subtract the approximate solution around the singularity. When using this method, the approximate function of ϕ is found about the singular point(s) (Igarashi & Honma, 1996; Lefeber, 1989). A new function, $\bar{\phi}$, is introduced and is given by ϕ and subtracting from that the approximate solution(s) found about the singular point(s) (Igarashi & Honma, 1996; Lefeber, 1989). This is also applied to the boundary conditions (Igarashi & Honma, 1996; Lefeber, 1989). BEM is used and there are additional unknowns that need to be found to find the coefficient(s) of the approximate solution(s) about the singular point(s) (Igarashi & Honma, 1996; Lefeber, 1989). Once those have been found, one can solve for ϕ (Igarashi & Honma, 1996; Lefeber, 1989). We prefer to do a hands on approach, described in the next paragraph.

Muleshkov (1988) introduced the idea and method of improving the BEM solution by replacing the linear function used to approximate the unknown variable (either ϕ or $\frac{\partial \phi}{\partial n}$) on the elements adjacent to singular points on the boundary by using the exact Conformal Mapping solution for a domain which is obtained by extending to infinity the sides that are adjacent to the singularity and preserving the original boundary condition that is valid around the singularity. The improvement from the exact solution is imposed in BEM to find the BEM solution improved by Conformal Mapping (Muleshkov, 1988). This hands on method of improving the solution by Conformal Mapping allows the local behavior of the exact solution found by Conformal Mapping to determine what is used

for ϕ or $\frac{\partial \phi}{\partial n}$, whichever is unknown, on the elements adjacent to the singularities rather than choosing as a guess to use linear, quadratic, cubic, etc interpolation used in some books.

This thesis will use the method given by Muleshkov (1988) first in a rectangle with a singular boundary. The need for improvement of BEM will be demonstrated by comparing the BEM solution to the exact solution. Then, the improvement of the BEM solution by Conformal Mapping will be compared to the exact solution and the BEM solution. This demonstration of the improvement of the BEM solution by Conformal Mapping will then be applied to a more complicated realistic finite domain with a very singular boundary. Some conclusions from our observations of the improvement of BEM by Conformal Mapping are given in Chapter 5.

Chapter 2. Explanation of the Conformal Mapping Method and BEM Used in this Thesis

2.1 Solving BVPs for the Two-Dimensional Laplace PDE by Conformal Mapping

An overview of solving BVPs for the Laplace PDE can be solved exactly by Conformal Mapping was given in Chapter 1.2. Since the Riemann Mapping Theorem does not provide the process for finding the conformal mapping of D onto D^*, in this section an overview of the techniques that will be used to find the conformal mapping of D onto D^* is given. The physical domain and its boundary are given in the $x-y$ plane where $z = x + iy$ with constant Dirichlet or zero Neumann Boundary conditions on various portions of the boundary.

There are different ways to find the function, $\omega = f(z)$, which conformally maps the physical domain in the $x-y$ plane onto its image in the $\phi-\psi$ plane, called the complex potential plane. The $\phi-\psi$ plane is constructed from the given boundary conditions. It is possible to prove that when $\frac{\partial\phi}{\partial n} = 0$, then $\psi = \text{const}$. In this thesis, one particular method is used. First, each domain, D and D^*, are conformally mapped onto upper half planes (Muleshkov, 2016). For instance, $\mathrm{w} = g(z)$, where $g(z)$ is an analytic function in D that maps conformally the domain in the $x-y$ plane onto the upper half plane of the $u-v$ plane where $\mathrm{w} = u + iv$ (Muleshkov, 2016). Similarly, $\zeta = h(\omega)$, where $h(\omega)$ is an analytic function in D^* that conformally maps D^* in the $\phi-\psi$ plane onto the upper half plane of the $\xi-\eta$ plane where $\zeta = \xi + i\eta$ (Muleshkov, 2016). Once D and D^* are conformally mapped onto upper half planes in the $u-v$ plane and $\xi-\eta$ plane respectively, a bilinear/linear function, $\zeta = \frac{A\mathrm{w}+B}{C\mathrm{w}+D}$,where A, B, C, and D are arbitrary real numbers and $AD \neq BC$, is used to conformally map the upper half plane in the $u-v$ plane onto the upper half plane in the $\xi-\eta$ plane (Muleshkov, 2016).

According to the Riemann Mapping Theorem, only three points are needed for $\zeta(\mathrm{w})$ to be unique. Therefore, A, B, C, or D could be chosen and then three corresponding points on the boundaries of the upper half planes in $u-v$ plane and $\xi-\eta$ plane are used to find the remaining constants. Once all constants have been found, $\omega = f(z)$ can be obtained.

Hence, the analytic function that maps D onto D^* is given by $\omega(z) = h^{-1}(\frac{Ag(z)+B}{Cg(z)+D})$. Next, two methods used in this thesis to find the conformal mappings, $g(z)$ and $h(\omega)$, are overviewed.

When the domain inside a generalized polygon is simple, such as not too many vertices and not too many portions of the boundary geometric transformations or elementary functions can be used. The geometric transformations are: translation, rotation, dilation, and opening of angles. To translate a domain to the left, right, up or down, one can add a complex number to z. To rotate the domain, one can multiply z by $\mathrm{e}^{\mathrm{i}\theta}$, where θ is the angle of rotation measured from the positive real axis. The domain can be dilated or shrunk by multiplying z by a positive real number. Lastly, if the boundary of the domain has at least two points, one can open or shrink the angle at the point by first moving the point to the origin, then by raising z to a power. In addition, elementary functions could be used to conformally map a domain inside a generalized polygon onto an upper half plane. The geometric transformations and elementary functions satisfy the conditions for the mapping to be a conformal mapping.

In the case that the domain is inside of a more difficult generalized polygon, the Schwarz-Cristoffel formula can be used to find the conformal mapping of the domain inside a generalized polygon onto an upper half plane. Actually, the Schwarz-Cristoffel formula can be used for a domain inside any generalized polygon (Carrier et al., 2005), but simpler methods as described above could be easier depending on the domain. The Schwarz-Cristoffel formula conformally maps the upper half plane in the $\xi-\eta$ plane where $\zeta = \xi + i\eta$ with boundary points $\xi_1 < \xi_2 < ... < \xi_n$ onto the interior of a generalized polygon in the $x - y$ plane where $z = x + iy$ and is given by

$$z = \bar{A} \int_{\zeta_o}^{\zeta} \prod_{k=1}^{n} (\zeta^* - \xi_k)^{\alpha_k - 1} d\zeta^* + \bar{B} \tag{8}$$

where α_k is the interior angle of z_k in the $x - y$ plane and $\overline{A}$ and $\overline{B}$ are constants that can be found from corresponding points from the generalized polygon and upper half plane. There are $n + 3$ unknowns in Eq. 8. From the Riemann Mapping Theorem, three

could be chosen arbitrarily for convenience. For instance, three parameters could be chosen or symmetry could be used which is the equivalent of one choosing one parameter (Muleshkov, 2016).

Hence, in order to find the conformal mapping of the domain inside a generalized polygon onto the upper half plane, Eq. 8 is used first to find the analytic function that conformally maps the domain in the upper half plane onto the domain inside the generalized polygon, then the inverse of the function that conformally maps the domain in the $x-y$ plane onto the upper half plane in the $\xi-\eta$ plane is found (Muleshkov, 2016).

In Chapter 3.2, the the conformal mapping of a domain inside a rectangle onto an upper half plane will be needed. Before it is shown how the domain inside of a rectangle is conformally mapped onto an upper half plane, some important properties of elliptic integrals and elliptic functions are needed.

The Incomplete Elliptic Integral of First Kind is

$$F(\xi, k) = \int_0^{\xi} \frac{d\zeta}{\sqrt{(1-\zeta^2)(1-k^2\zeta^2)}} \tag{9}$$

where k is referred to as the modulus and $k\epsilon(0,1)$ and $k' = \sqrt{1-k^2}$.

The Complete Elliptical Integral of First Kind is

$$F(1, k) = \int_0^{1} \frac{dz}{\sqrt{(1-z^2)(1-k^2z^2)}} = K(k) \tag{10}$$

and using Eq. 10, if there is k' instead of k one gets,

$$K'(k) = K(k') \tag{11}$$

Lastly, The Elliptic Sine Function is

$$\xi = \mathrm{sn}(z, k) \tag{12}$$

which is the inverse of $z = F(\xi, k)$.

Now, to find the conformal mapping of a domain inside a rectangle onto an upper half

plane, without loss of generality, a rectangle with the horizontal lower base centered at the origin with length $2a$ and height b can be considered and is shown in Figure 1a. The domain in Figure 1a needs to be conformally mapped onto the upper half plane in Figure 1b. In Figure 1b, two parameters (A and B) have been chosen as well as a symmetry (C and D).

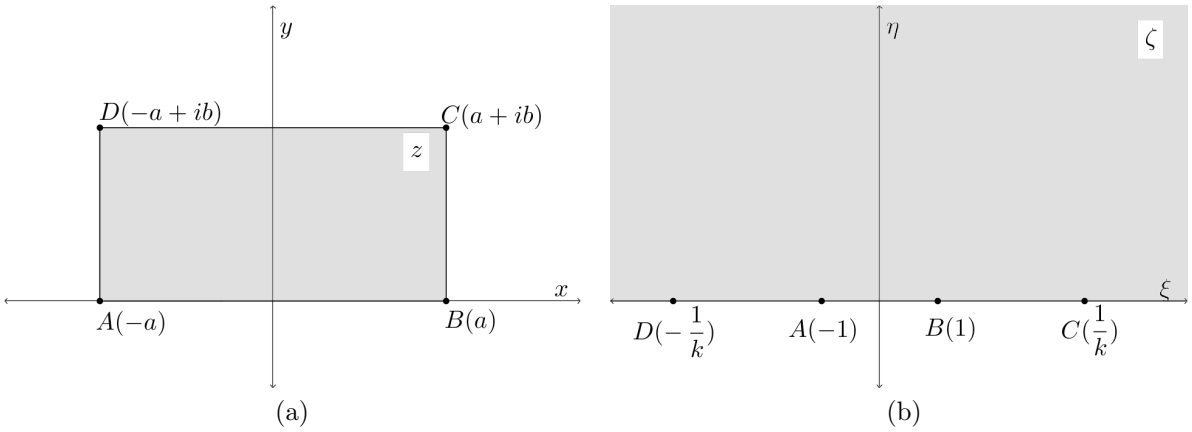

Figure 1: (a) Domain Inside a Rectangle in the $x - y$ plane (b) Upper half Plane in the $\xi - \eta$ plane

Using Eq. 10 to conformally map the upper half plane in Figure 1b onto the domain in Figure 1a, one gets,

$$z = \bar{A} \int_0^{\zeta} \frac{d\zeta^*}{\sqrt{(1 - (\zeta^*)^2)(1 - k^2(\zeta)^{*2})}} + \bar{B} \tag{13}$$

Then, using points corresponding points A and B in Figure 1b and 1a to find $\bar{A}$ and $\bar{B}$ to obtain

$$\bar{A} = \frac{a}{K(k)} \tag{14}$$

and

$$\bar{B} = 0 \tag{15}$$

Thus, Eq. 13 becomes

$$z = \frac{a}{K(k)} \int_0^{\zeta} \frac{d\zeta^*}{\sqrt{(1-(\zeta)^{*2})(1-k^2(\zeta)^{*2})}} = \frac{a}{K(k)} F(\zeta, k) \tag{16}$$

Using corresponding points C and D in Figure 1b and 1a to obtain

$$\frac{K^{'}(k)}{K(k)} = \frac{b}{a} \tag{17}$$

and the approximate value of k can be found using the tables in "Handbook of Mathematical Functions" by Abramowitz and Stegun (Muleshkov, 2016).

Eq. 13 is a doubly multivalued function, so for the conformal mapping, a particular branch is chosen so that the upper half plane in the $\xi - \eta$ plane is mapped conformally onto the interior of the rectangle in the $x - y$ plane (Muleshkov, 2016). On the other hand, the goal is to find an analytic function that conformally maps the domain inside the rectangle in Figure 1a onto the upper half plane in Figure 1b. To do this, the inverse of Eq. 13 is needed, which is the Elliptic Sine Function given by

$$\zeta = \mathrm{sn}(\frac{K(k)}{a} z, k) \tag{18}$$

which is a doubly periodic elliptic function.

In sum, to find the exact solution of BVPs for the two-dimensional Laplace PDE inside a generalized polygon by Conformal Mapping with the conditions given in Chapter 1.2, using either geometric transformation(s) or the Schwarz-Cristoffel formula, the domain and its image are conformally mapped onto upper half planes. Then, using a bilinear function and three corresponding points on the boundaries of the upper half planes, one can find the conformal mapping , $\omega = f(z)$, of D onto D^*. The real part, $\phi(x, y)$, of $f(z)$, is the exact solution of BVPs for the two-dimensional Laplace PDE in the domain.

2.2 Flow Net

Once the conformal mapping, $\omega = f(z) = \phi(x, y) + i\psi(x, y)$, has been found by the methods described in Chapter 2.1, the real and imaginary parts are used to find the equipotential lines and streamlines of the flow. When $\phi(x, y) = \hat{C}$, where $\phi_{min} <$

$\hat{C} < \phi_{max}$ is a constant, the lines are called equipotential lines (Harr, 1990). When $\psi(x, y) = C^*$, where C^* is a constant, the lines are called streamlines (Harr, 1990). The set of the equipotential lines and streamlines is called the flow net. When the flow net is drawn, the streamlines and equipotential lines intersect at an angle of $\frac{\pi}{2}$ in the domain (Harr, 1990; Mathews & Howell, 2012). This property of the equipotential lines and streamlines is one way to observe the impact of improving BEM using Conformal Mapping.

2.3 Governing Equations for Finding the BEM Solution

In Chapter 1.2, an overview of BEM was provided. In this section, the equations to find the BEM solution are developed.

If $U(x, y)$ and $V(x, y)$ are twice differentiable functions, in a given domain, D, with boundary Γ, then $U(x, y)$ and $V(x, y)$ satisfy Green's Second Identity

$$\int\int_D (U\nabla^2 V - V\nabla^2 U)dxdy = \oint_\Gamma (U\frac{\partial V}{\partial n} - V\frac{\partial U}{\partial n})ds \tag{19}$$

where $\frac{\partial V}{\partial n}$ and $\frac{\partial U}{\partial n}$ are the normal derivatives of $V(x, y)$ and $U(x, y)$ respectively.

If $U(x, y)$ and $V(x, y)$ satisfy the Laplace PDE then, $\Delta U = \Delta V = 0$. $U(x, y)$ and $V(x, y)$ are chosen to be:

$U(x, y) = \phi(x, y)$

$V(x, y) = \ln r_p$

where $V(x, y)$ can be found from the Fundamental Solution of Green's Function for the two-dimensional Laplace PDE and $r_p = \sqrt{(x - x_p)^2 + (y - y_p)^2}$ is the distance from any point (x, y) to any fixed point $p = (x_p, y_p)$. Hence, Eq. 19 becomes

$$\oint_\Gamma (\frac{\phi}{r_p} \cdot \frac{\partial r_p}{\partial n} - \frac{\partial \phi}{\partial n} \ln r_p)ds = 0 \tag{20}$$

When $(x_p, y_p) = (x, y)$, then $r_p = 0$ which is a singularity of the integrand in Eq. 20. (Liggett & Liu, 1983; Muleshkov, 1988). So, evaluating the integral in Eq. 20 as the principle value, Eq. 20 becomes

$$\oint_{\Gamma}(\frac{\phi}{r_p}\cdot\frac{\partial r_p}{\partial n}-\frac{\partial\phi}{\partial n}\ln r_p)ds=\alpha_p\phi_p \tag{21}$$

where α_p is determined by the location of p. If p is on Γ, then α_p is the angle between the segments adjacent to p (Liggett & Liu, 1983). Hence, if p is on a smooth part of the boundary, $\alpha_p=\pi$. If p is in the domain, then α_p is equal to 2π.

Given that the boundary, Γ, is discretized into segments with end points $s=s_m$ and $s=s_{m+1}$, Eq. 21 becomes

$$\int_{s_m}^{s_{m+1}}(\frac{\phi}{r_p}\cdot\frac{\partial r_p}{\partial n}-\frac{\partial\phi}{\partial n}\ln r_p)ds+\int_{s_{m+1}}^{s_{m+2}}(\frac{\phi}{r_p}\cdot\frac{\partial r_p}{\partial n}-\frac{\partial\phi}{\partial n}\ln r_p)d+...-\alpha_p\phi_p=0 \tag{22}$$

with m and p going 1 to N. Eq. 22 can be written as

$$\sum_{m=1}^{N}I_{m,m+1}^{(p)}-\alpha_p\phi_p=0\,,\ p=1,2,3,...N \tag{23}$$

where

$$I_{m,m+1}^{(p)}=\int_{s_m}^{s_{m+1}}(\frac{\phi}{r_p}\cdot\frac{\partial r_p}{\partial n}-\frac{\partial\phi}{\partial n}\ln r_p)ds \tag{24}$$

(Muleshkov, 1988).

When ϕ is given, $\frac{\partial\phi}{\partial n}$ is approximated by a linear function found by linear interpolation between two nodes where the values of the normal derivative at the nodes are unknown and sought. On elements where $\frac{\partial\phi}{\partial n}$ is given, ϕ is approximated by a linear function found by linear interpolation between two nodes where the values of ϕ at the nodes are unknown and sought. To find the linear interpolation between two nodes on an element, the element has end points or nodes of $s=s_m$ and $s=s_{m+1}$. The unknown value at a node is denoted by Ω_m and corresponds to either ϕ or $\frac{\partial\phi}{\partial n}$ (whichever is unknown). Using the linear interpolation function, the unknown variable (ϕ or $\frac{\partial\phi}{\partial n}$), Ω, on an element is given by,

$$\Omega=\Omega_m\cdot\frac{(s_{m+1}-s)}{(s_{m+1}-s_m)}+\Omega_{m+1}\cdot\frac{(s-s_m)}{(s_{m+1}-s_m)} \tag{25}$$

Then, evaluating Eq. 24 from $m-1$ to m and using Eq. 25 one gets,

$$I^{(p)}_{m-1,m} = \Omega_{m-1} \cdot a^{(m-1)}_{p,m-1} + \Omega_m \cdot a^{(m-1)}_{p,m} + B_{p,m-1} \tag{26}$$

where $a^{(m-1)}_{p,m-1}$ is the coefficient of Ω_{m-1}, $a^{(m-1)}_{p,m}$ is the coefficient of Ω_m, and $B_{p,m-1}$ is the evaluated integral containing the known constant, all found from the evaluation of the $m-1$th integral in Eq. 24.

Similarly, when evaluating Eq. 24 from m to $m+1$ using Eq. 25 one gets,

$$I^{(p)}_{m,m+1} = \Omega_m \cdot a^{(m)}_{p,m} + \Omega_{m+1} \cdot a^{(m)}_{p,m+1} + B_{p,m} \tag{27}$$

where $a^{(m)}_{p,m}$ is the coefficient of Ω_m, $a^{(m)}_{p,m+1}$ is the coefficient of Ω_{m+1}, and $B_{p,m}$ is the evaluated integral containing the known constant, all found from the evaluation of the mth integral in Eq. 24.

Using,

$$\delta_p = \begin{cases} 1 & \phi_p \, is \, unknown \\ 0 & \phi_p \, is \, known \end{cases}$$

From Eq. 26 and Eq. 27 the coefficient of Ω_m, $A_{p,m}$, can be written as

$$A_{p,m} = a^{(m-1)}_{p,m} + a^{(m)}_{p,m} - \delta_p \alpha_p \phi_p \tag{28}$$

and the values from integrals that result in either ϕ or $\frac{\partial \phi}{\partial n}$ being known on an element are written as

$$B_p = \alpha_p (1 - \delta_p) \phi_p - \sum_{m=1}^{N} B_{p,m} \tag{29}$$

where p goes from 1 to N (Muleshkov, 1988).

Thus, Eq. 28 and Eq. 29 lead to a system of linear equations,

$$\sum_{m=1}^{N} A_{p,m} \Omega_m = B_p \tag{30}$$

where p goes from 1 to N (Muleshkov, 1988).

Using matrix form, Eq. 30 can be written as

$$[A]_{N,N}[\Omega]_{N,1} = [B]_{N,1} \tag{31}$$

(Muleshkov, 1988).

When the integral formula for $a_{p,m}^{(m)}$ is known and given by

$$a_{p,m}^{(m)} = I(x_m, x_{m+1}, y_m, y_{m+1,....}) \tag{32}$$

then the formula for $a_{p,m}^{(m-1)}$ can be obtained by placing $m+1$ by $m-1$ and making the integral negative,

$$a_{p,m}^{(m-1)} = -I(x_m, x_{m-1}, y_m, y_{m-1,....}) \tag{33}$$

(Muleshkov, 1988).

When calculating $A_{p,m}$, it is helpful to find $a_{p,m}^{(m)}$ then use Eq. 33 to obtain $a_{p,m}^{(m-1)}$.

Once BEM is used to find all of the unknown values on the boundary at the chosen nodes by the system in Eq. 31, the solution of ϕ at a specific point, p, inside the domain is found by using Eq. 21,

$$2\pi\phi_p = \oint_{\Gamma} (\frac{\phi}{r_p} \cdot \frac{\partial r_p}{\partial n} - \ln r_p \cdot \frac{\partial \phi}{\partial n}) ds \tag{34}$$

where now all values of ϕ and $\frac{\partial \phi}{\partial n}$ are known at the chosen nodes. Eq. 34 is used to find the potential at a point, p, inside the domain.

Chapter 3. Demonstration of Solving a BVP for the Two-Dimensional Laplace PDE inside a Rectangle with a Singular Boundary

3.1 Example 1

In order to demonstrate the need for improvement of the BEM solution of the two-dimensional Laplace PDE for two dimensional underground water flow as described in Chapter 1.1 in a domain with a singular boundary, a domain inside a rectangle with a singular boundary is considered first. Since the exact solution of a BVP for the two-dimensional Laplace PDE inside a rectangle can be found, the BEM solution (Chapter 3.2) and the improved BEM solution (Chapter 3.5) can be compared to the exact solution.

Example 1. Solve the BVP for the Laplace PDE with the following boundary conditions:

On AE, $\phi(x,0) = 0, \quad -l < x < \sigma$

On EB, $\frac{\partial \phi}{\partial n}(x,0) = 0, \quad \sigma < x < l$

On BC, $\phi(l,y) = 1, \quad 0 < y < l$

On CD, $\phi(x,l) = 1, \quad -l < x < l$

On DA, $\phi(l,y) = 1, \quad 0 < y < l$

where $-l < \sigma < l$. When solving the problem, the values of l and σ are chosen. The physical domain of the problem is shown in Figure 2.

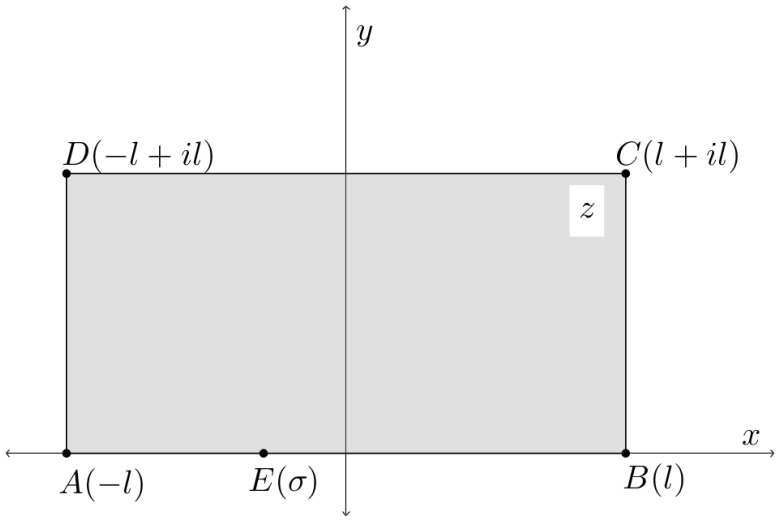

Figure 2: Physical Domain of Example 1 in the $x - y$ plane

Note that $\phi(x,y) = 1$ is the same as the maximum potential (ϕ_{max}) and $\phi(x,y) = 0$ is the same as the minimum potential (ϕ_{min}). These values are found by using by subtracting

the value of the minimum potential from the value of the maximum potential and dividing by the value of the minimum potential .

The singular points of the domain in Figure 2 are points A, E, C, and D. At point A, the entrance and exit of the flow try to meet at one in the same point. At point E, the insulated portion and the free exit meet at π rather than $\frac{\pi}{2}$. At points C and D, the same potential meets at $\frac{\pi}{2}$. Point B is not a singular point since $\frac{\partial \phi}{\partial n} = 0$ and $\phi = 1$ meet at angle $\frac{\pi}{2}$.

The complex potential plane of the domain in Figure 2 is shown in Figure 3.

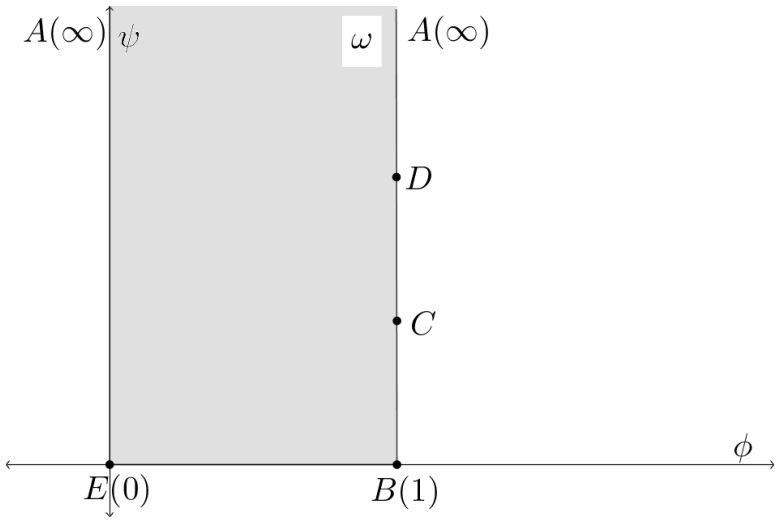

Figure 3: Complex Potential Plane of Example 1 in the $\phi - \psi$ plane

3.2 Exact Solution of Example 1 by Conformal Mapping

In this section, Example 1 will be solved exactly by Conformal Mapping using the techniques described in Chapter 2.1.

First, the domain in the $x - y$ plane shown in Figure 2 is shrunk by using

$$z_1 = \frac{K(k)}{l} z \tag{35}$$

where $z_1 = x_1 + iy_1$ and the domain in the $x_1 - y_1$ plane is shown in Figure 4a.

From Eq. 17, $\frac{K'(k)}{K(k)} = 1$ which gives $k = \frac{1}{\sqrt{2}}$ (Abramowitz & Stegun, 2013). Thus, Eq. 35 becomes

$$z_1 = \frac{K(\frac{1}{\sqrt{2}})}{l} z \tag{36}$$

Next, to conformally map the domain in the $x_1 - y_1$ plane in Figure 4a onto the upper half plane in Figure 4b, one uses Eq. 12 to obtain

$$z_2 = \mathrm{sn}(z_1, \frac{1}{\sqrt{2}}) \tag{37}$$

where $z_2 = x_2 + iy_2$. Therefore, from Eq. 36 and Eq. 37, the analytic function that conformally maps the domain inside the rectangle from Example 1 onto the upper half plane is given by

$$z_2 = \mathrm{sn}(\frac{K(\frac{1}{\sqrt{2}})}{l} z, \frac{1}{\sqrt{2}}) \tag{38}$$

Next, the complex potential plane in the $\phi - \psi$ plane shown in Figure 3 is conformally mapped onto an upper half plane.

First, the domain in the $\phi - \psi$ plane is mapped onto a quarter plane by using

$$\omega_1 = \sin\frac{\pi}{2}\omega \tag{39}$$

where $\omega_1 = \phi_1 + i\psi_1$, and the domain in the $\phi_1 - \psi_1$ plane is shown in Figure 5a.

Then, to conformally map the domain in the $\phi_1 - \psi_1$ plane in Figure 5a onto the upper half plane in Figure 5b, the angle is opened,

$$\omega_2 = \omega_1^2 \tag{40}$$

where $\omega_2 = \phi_2 + i\psi_2$.

Therefore, the equation that maps the complex potential plane onto the upper half plane in Figure 5b is given by

$$\omega_2 = \sin^2\frac{\pi}{2}\omega = \frac{1 - \cos\pi\omega}{2} \tag{41}$$

The bilinear function which conformally maps the domain in the $x_2 - y_2$ plane onto

the upper half plane in the $\phi_2 - \psi_2$ plane is given by

$$\omega_2 = \frac{Pz_2 + Q}{Rz_2 + S} \tag{42}$$

where P, Q, R, and S are arbitrary real numbers. From the Riemann Mapping Theorem, one parameter can be chosen, so let $R = 1$. Using corresponding points A, B, and, E in Figure 4b and 5b, one gets, $P = \frac{2}{1-\hat{\sigma}}$, $Q = \frac{-2\hat{\sigma}}{1-\hat{\sigma}}$, and $S = 1$. Thus, Eq. 42 becomes,

$$\omega_2 = \frac{2(z_2 - \hat{\sigma})}{(1-\hat{\sigma})(z_2 + 1)} \tag{43}$$

where $\hat{\sigma}$ is found from Eq. 38 and is given by

$$\hat{\sigma} = \mathrm{sn}(\frac{K(\frac{1}{\sqrt{2}})}{l}\sigma, \frac{1}{\sqrt{2}}) \tag{44}$$

By Using Eq. 44, Eq. 38, in Eq. 43, the function, $\omega = f(z)$ is obtained

$$\omega = \frac{1}{\pi}\arccos(\frac{-4(\mathrm{sn}(\frac{K(\frac{1}{\sqrt{2}})}{l}z, \frac{1}{\sqrt{2}}) - \mathrm{sn}(\frac{K(\frac{1}{\sqrt{2}})}{l}\sigma, \frac{1}{\sqrt{2}}))}{(1 - \mathrm{sn}(\frac{K(\frac{1}{\sqrt{2}})}{l}\sigma, \frac{1}{\sqrt{2}}))(\mathrm{sn}(\frac{K(\frac{1}{\sqrt{2}})}{l}z, \frac{1}{\sqrt{2}}) + 1)} + 1) \tag{45}$$

as the analytic function inside the domain that conformally maps the domain in Figure 2 to the domain in Figure 3.

Since, $\omega = f(z) = \phi(x, y) + i\psi(x, y)$, the solution of the BVP given in Example 1 is

$$\phi(x, y) = \mathrm{Re}[\frac{1}{\pi}\arccos\frac{-4(\mathrm{sn}(\frac{K(\frac{1}{\sqrt{2}})}{l}z, \frac{1}{\sqrt{2}}) - \mathrm{sn}(\frac{K(\frac{1}{\sqrt{2}})}{l}\sigma, \frac{1}{\sqrt{2}}))}{(1 - \mathrm{sn}(\frac{K(\frac{1}{\sqrt{2}})}{l}\sigma, \frac{1}{\sqrt{2}}))(\mathrm{sn}(\frac{K(\frac{1}{\sqrt{2}})}{l}z, \frac{1}{\sqrt{2}}) - 1)} + 1] \tag{46}$$

and a representation of the solution, the equipotential lines, is given in Chapter 3.3 and Chapter 3.6

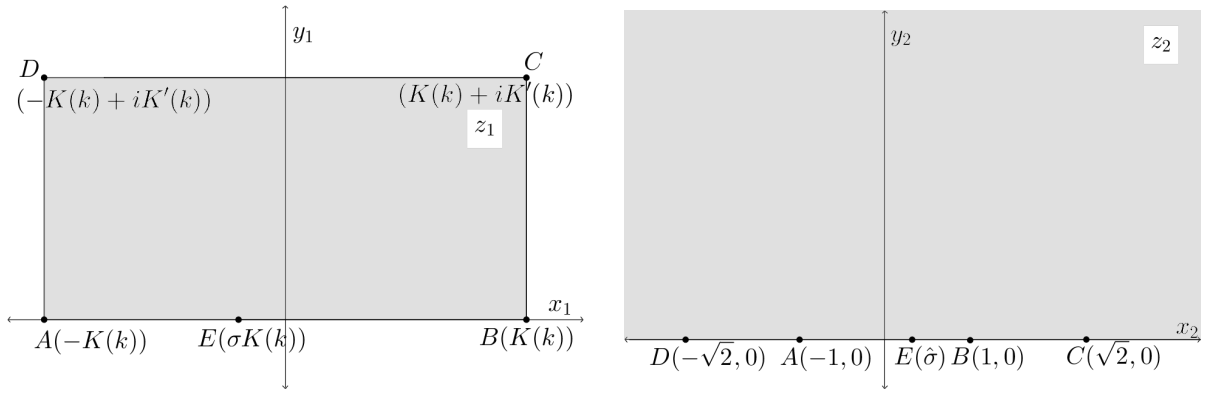

(a) (b)

Figure 4: (a) $x_1 - y_1$ plane (b) $x_2 - y_2$ plane

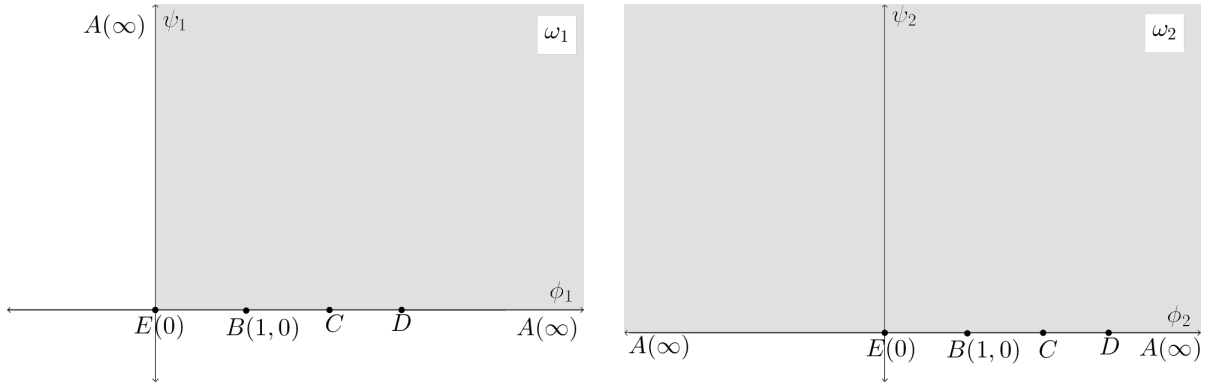

(a) (b)

Figure 5: (a) $\phi_1 - \psi_1$ plane (b) $\phi_2 - \psi_2$ plane

3.3 BEM Solution of Example 1

In order to use BEM as outlined in Chapter 1.2 to find the solution, $\phi(x, y)$, of Example 1, the boundary of the domain given in Example 1 and shown in Figure 2 needs to be discretized. The boundary of the domain in Figure 2 is discretized as follows: AE is discretized into k_1 elements, EB is discretized into k_2 elements, BC is discretized into k_3 elements, CD is discretized into k_4 elements, and lastly, DA is discretized into k_5 elements. Instead of having a node at each point A, C, and D, two nodes approach each point thus using discontinuous elements adjacent to A, C, and D. Through experimentation, it was discovered that there is no need to use two nodes that approach point E instead of a node at point E. Thus, total number of nodes is $N = k_1 + k_2 + k_3 + k_4 + k_5 + 3$, and the choice of the numbering of the nodes begins at the first node after point A. For notation, $K1 = k_1, K2 = k_1 + k_2, ..., K5 = k_1 + k_2 + k_3 + k_4 + k_5$.

The integrals from Eq. 24 on each portion of the boundary are developed in this section. Then, what is needed to solve the system in Eq. 31 is found by using Eq. 28 and Eq. 29. All the integrals that come from Eq. 24 on each portion of the boundary are defined and solved in Appendix A.

On the portion of the boundary AE,

$y = 0$ and $-l + \epsilon_1 < x < \sigma$ where ϵ_1 is the distance after point A.

$\phi(x, 0) = 0$

$\frac{\partial \phi}{\partial n}(x, 0) = \Omega = \Omega_m(\frac{x_{m+1}-x}{x_{m+1}-x_m}) + \Omega_{m+1}(\frac{x-x_m}{x_{m+1}-x_m})$

$r_p = \sqrt{(x - x_p)^2 + y_p^2}$

From Eq. 24, one gets

$$I^{(p)}_{m,m+1} = -\Omega_m \int_{x_m}^{x_{m+1}} (\frac{x_{m+1} - x}{x_{m+1} - x_m}) \ln \sqrt{(x - x_p)^2 + y_p^2} dx -$$

$$\Omega_{m+1} \int_{x_m}^{x_{m+1}} (\frac{x - x_m}{x_{m+1} - x_m}) \ln \sqrt{(x - x_p)^2 + y_p^2} dx \tag{47}$$

for two nodes, m and $m + 1$, on AE.

Therefore, from Eq. 47,

$$a_{p,m}^{(m)} = -I_1(x_m, x_{m+1}, x_p, y_p) \tag{48}$$

and from Eq. 33

$$a_{p,m}^{(m-1)} = I_1(x_m, x_{m-1}, x_p, y_p) \tag{49}$$

There is no contribution to B_p from Eq. 47.

On the portion of the boundary EB,

$\sigma < x < l$ and $y = 0$

$\phi(x,0) = \Omega = \Omega_m(\frac{x_{m+1}-x}{x_{m+1}-x_m}) + \Omega_{m+1}(\frac{x-x_m}{x_{m+1}-x_m})$

$\phi(l,0) = \frac{x-x_{K2}}{x_{K2+1}-x_{K2}}$

$\frac{\partial\phi}{\partial n}(x,0) = 0$

$r_p = \sqrt{(x-x_p)^2 + y_p^2}$

$\frac{\partial r_p}{\partial n}(x,0) = \frac{y_p}{r_p}$

From Eq. 24 one gets,

$$I_{m,m+1}^{(p)} = \int_{x_{K2}}^{x_{K2+1}} (\frac{x-x_{K2}}{x_{K2+1}-x_{K2}}) \cdot \frac{y_p}{(x-x_p)^2+y_p^2} dx -$$

$$\Omega_m \int_{x_m}^{x_{m+1}} (\frac{x_{m+1}-x}{x_{m+1}-x_m}) \cdot \frac{y_p}{(x-x_p)^2+y_p^2} dx -$$

$$\Omega_{m+1} \int_{x_m}^{x_{m+1}} (\frac{x-x_m}{x_{m+1}-x_m}) \cdot \frac{y_p}{(x-x_p)^2+y_p^2} dx \tag{50}$$

for two nodes, m and $m+1$, on EB.

Therefore, from Eq. 50

$$a_{p,m}^{(m)} = I_2(x_m, x_{m+1}, x_p, y_p) \tag{51}$$

and from Eq. 33

$$a_{p,m}^{(m-1)} = -I_2(x_m, x_{m-1}, x_p, y_p) \tag{52}$$

There is a contribution to $B_{p,m}$ from $m = K2 + 1$ from Eq. 50 given by

$$B_{p,K2+1} = -I_2(x_{K2+1}, x_{K2}, x_p, y_p) \tag{53}$$

On the portion of the boundary BC,

$x = l$ and $0 < y < l - \epsilon_2$ where ϵ_2 is the distance before C.

$\phi(l, y) = 1$

$\frac{\partial \phi}{\partial n}(l, y) = \Omega = \Omega_m(\frac{y_{m+1}-y}{y_{m+1}-y_m}) + \Omega_{m+1}(\frac{y-y_m}{y_{m+1}-y_m})$

$r_p = \sqrt{(y - y_p)^2 + (l - x_p)^2}$

$\frac{\partial r_p}{\partial n} = \frac{l-x_p}{r_p}$

From Eq. 24 one gets,

$$I_{m,m+1}^{(p)} = \int_{y_m}^{y_{m+1}} \frac{l - x_p}{(y - y_p)^2 + (l - x_p)^2} dy -$$

$$\Omega_m \int_{y_m}^{y_{m+1}} (\frac{y_{m+1} - y}{y_{m+1} - y_m}) \ln \sqrt{(y - y_p)^2 + (l - x_p)^2} dy \; -$$

$$\Omega_{m+1} \int_{y_m}^{y_{m+1}} (\frac{y - y_m}{y_{m+1} - y_m}) \ln \sqrt{(y - y_p)^2 + (l - x_p)^2} dy \tag{54}$$

for two nodes, m and $m + 1$, on BC.

Therefore, from Eq. 54

$$a_{p,m}^{(m)} = -I_1(y_m, y_{m+1}, y_p, l - x_p) \tag{55}$$

and from Eq. 33

$$a_{p,m}^{(m-1)} = I_1(y_m, y_{m-1}, y_p, l - x_p) \tag{56}$$

$B_{p,m}$ on BC is obtained from Eq. 54 and given by

$$B_{p,m} = I_3(y_{K2+1}, y_{K3+1}, y_p, l - x_p) \tag{57}$$

On the portion of the boundary CD,

$y = l$ and $-l + \epsilon_4 < x < l - \epsilon_3$ where ϵ_3 is the distance after C and ϵ_4 is the distance before D.

$\phi(x, l) = 1$

$\frac{\partial \phi}{\partial n}(x, l) = \Omega = \Omega_m(\frac{x_{m+1} - x}{x_{m+1} - x_m}) + \Omega_{m+1}(\frac{x - x_m}{x_{m+1} - x_m})$

$r_p = \sqrt{(x - x_p)^2 + (l - y_p)^2}$

$\frac{\partial r_p}{\partial n} = \frac{l - y_p}{r_p}$

From Eq. 24 one gets,

$$I_{m,m+1}^{(p)} = -\int_{x_m}^{x_{m+1}} \frac{l - y_p}{(x - x_p)^2 + (l - y_p)^2} dx +$$

$$\Omega_m \int_{x_m}^{x_{m+1}} (\frac{x_{m+1} - x}{x_{m+1} - x_m}) \ln \sqrt{(x - x_p)^2 + (l - y_p)^2} dx +$$

$$\Omega_{m+1} \int_{x_m}^{x_{m+1}} (\frac{x - x_m}{x_{m+1} - x_m}) \ln \sqrt{(x - x_p)^2 + (l - y_p)^2} dx \tag{58}$$

for two nodes, m and $m + 1$, on CD.

Therefore, from Eq. 58

$$a_{p,m}^{(m)} = I_1(x_m, x_{m+1}, x_p, l - y_p) \tag{59}$$

and from Eq. 33

$$a_{p,m}^{(m-1)} = -I_1(x_m, x_{m-1}, x_p, l - y_p) \tag{60}$$

for two nodes, m and $m+1$, on CD.

$B_{p,m}$ on CD is obtained from Eq. 58 and given by

$$B_{p,m} = I_3(x_{K4+2}, x_{K3+2}, x_p, l - y_p) \tag{61}$$

On portion of the boundary DA,

$x = -l$ and $\epsilon_6 < y < l - \epsilon_5$, where ϵ_5 is the distance after point D and ϵ_6 is the distance before point A.

$\phi(-l, y) = 1$

$\frac{\partial \phi}{\partial n}(-l, y) = \Omega = \Omega_m(\frac{y_{m+1}-y}{y_{m+1}-y_m}) + \Omega_{m+1}(\frac{y-y_m}{y_{m+1}-y_m})$

$r_p = \sqrt{(y - y_p)^2 + (l + x_p)^2}$

$\frac{\partial r_p}{\partial n} = \frac{l+x_p}{r_p}$

From Eq. 24, one gets,

$$I_{m,m+1}^{(p)} = -\int_{y_m}^{y_{m+1}} \frac{l + x_p}{(y - y_p)^2 + (l + x_p)^2} dy +$$

$$\Omega_m \int_{y_m}^{y_{m+1}} (\frac{y_{m+1} - y}{y_{m+1} - y_m}) \ln \sqrt{(y - y_p)^2 + (l + x)^2} dy$$

$$+\Omega_{m+1} \int_{y_m}^{y_{m+1}} (\frac{y - y_m}{y_{m+1} - y_m}) \ln \sqrt{(y - y_p)^2 + (l + x_p)^2} dy \tag{62}$$

for two nodes, m and $m+1$, on DA.

Therefore, from Eq. 62

$$a_{p,m}^{(m)} = I_1(y_m, y_{m+1}, y_p, l + x_p) \tag{63}$$

and from Eq. 33

$$a_{p,m}^{(m-1)} = -I_1(y_m, y_{m-1}, y_p, l + x_p) \tag{64}$$

for two nodes, m and $m+1$, on DA.

$B_{p,m}$ on DA is obtained from Eq. 62 and given by

$$B_{p,m} = I_3(y_{K5+3}, y_{K4+3}, y_p, l + x_p) \tag{65}$$

Therefore, using Eqs. 48-65 the matrices $[A]_{N,N}$ and $[B]_{N,1}$ are formed to solve the system in Eq. 31 to find the missing values at the chosen nodes. Then, using the values found from solving the system in Eq. 31 in Eq. 34 to find the potential, $\phi(x, y)$, in the domain, thus solving the BVP in Example 1.

3.4 Comparison of the Exact Solution to the BEM Solution of Example 1

In this section, the exact solution of $\phi(x, y)$ and the BEM solution of $\phi(x, y)$ to the problem given in Example 1 are compared. For the comparison, the following are chosen: $l = 1$, $\sigma = 0.25$, $k_1 = 10$, $k_2 = 70$, $k_3 = 40$, $k_4 = 80$, $k_5 = 40$, and $\epsilon_1 = \epsilon_2 = \epsilon_3 = \epsilon_4 = \epsilon_5 = \epsilon_6 = 0.0001$.

The equipotential lines, which solve the BVP in Example 1, are shown in Figure 6. The equipotential lines shown are from $\phi(x, y) = 0.1$ to $\phi(x, y) = 0.9$ in increments of 0.1.

From Figure 6, it is clear that the BEM solution of the BVP in Example 1 can be improved. Figure 7 shows more detail of one in the same equipotential line ($\phi(x, y) = 0.8$) from Figure 6. Table 1 shows some $x-$ values to the corresponding $y-$ values on $\phi(x, y) = 0.8$ from the exact solution and the BEM solution. Note that in Mathematica (Wolfram Research, Inc., 2018), the corresponding points on each line must be found manually, which is the reason only a few corresponding points are given in Table 1.

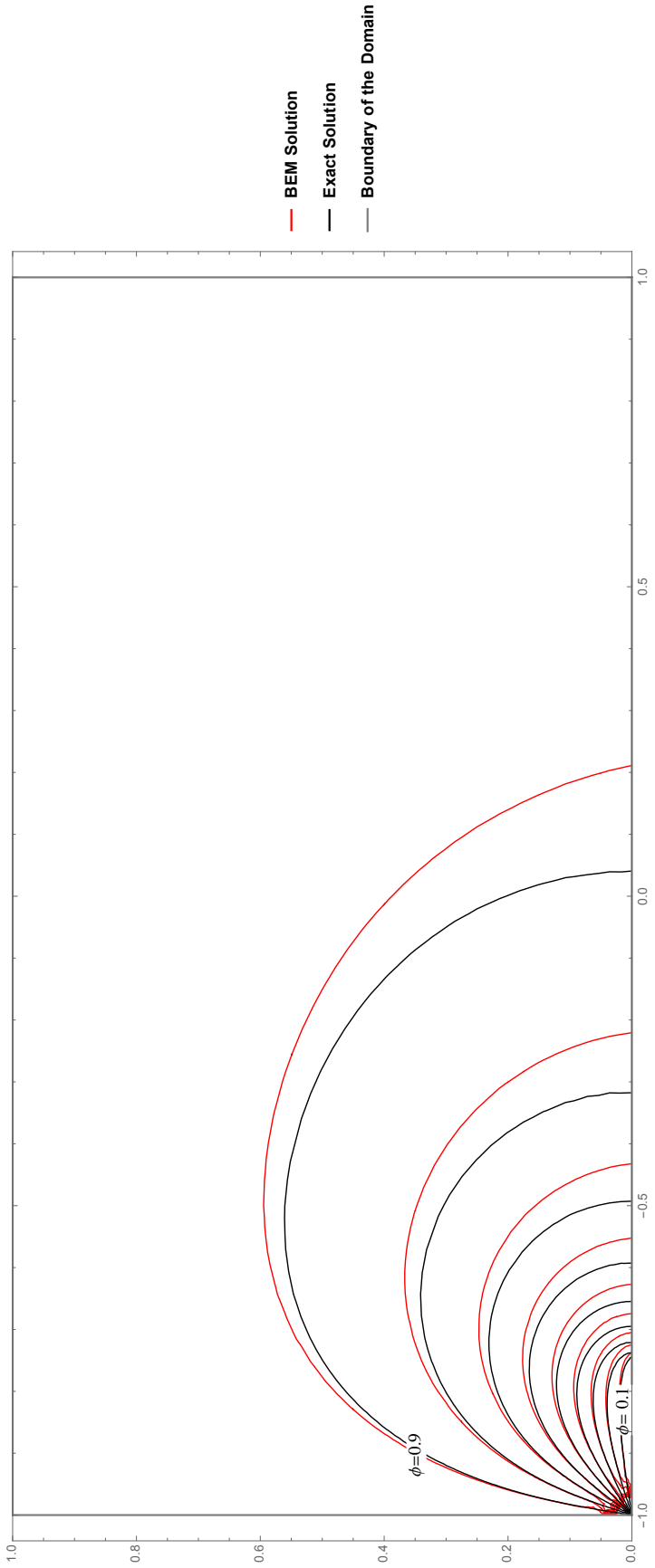

Figure 6: Solution by Conformal Mapping and BEM of Example 1

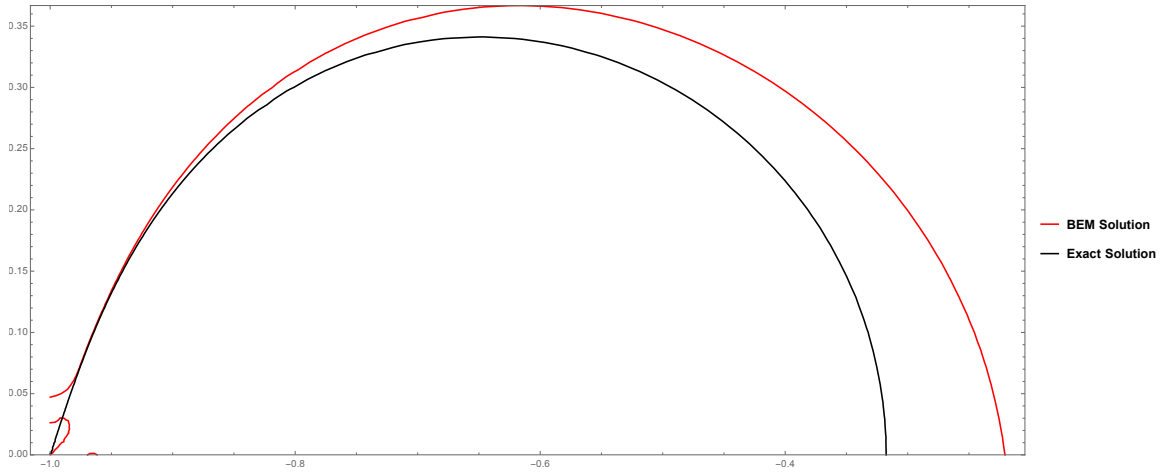

Figure 7: $\phi(x, y) = 0.8$ from the Exact Solution and the BEM solution

x	y (Exact Solution)	y (BEM Solution)	Difference of y
-0.3187	0.011	0.2221	0.2111
-0.3218	0.04964	0.2249	0.17526
-0.3252	0.06792	0.2303	0.16238
-0.3284	0.08242	0.2337	0.15128

Table 1: Selected Values on $\phi(x, y) = 0.8$ from the Exact Solution and the BEM Solution

Now that it been observed that the BEM solution for $\phi(x, y)$ in Example 1 can be improved, the method of improving the BEM solution by Conformal Mapping is shown in the next section, Chapter 3.5.

3.5 Conformal Mapping Improvement of the BEM Solution in Example 1

An overview of using Conformal Mapping to improve the BEM solution was provided in Chapter 1.2. In this section, that method is applied to every singular point on the boundary of the domain given in the problem in Example 1. All details are given for point A. For subsequent points, an overview is given as well as the improved contribution to find $A_{p,m}$ or B_p to solve the system in Eq. 31.

Point A

To determine the local behavior of $\frac{\partial \phi}{\partial n}$ near point A, the sides from point A in Figure 2 are extended to infinity preserving the given boundary condition valid near point A as shown in Figure 8a. The corresponding complex potential plane for the domain in Figure 8a is given in Figure 8b.

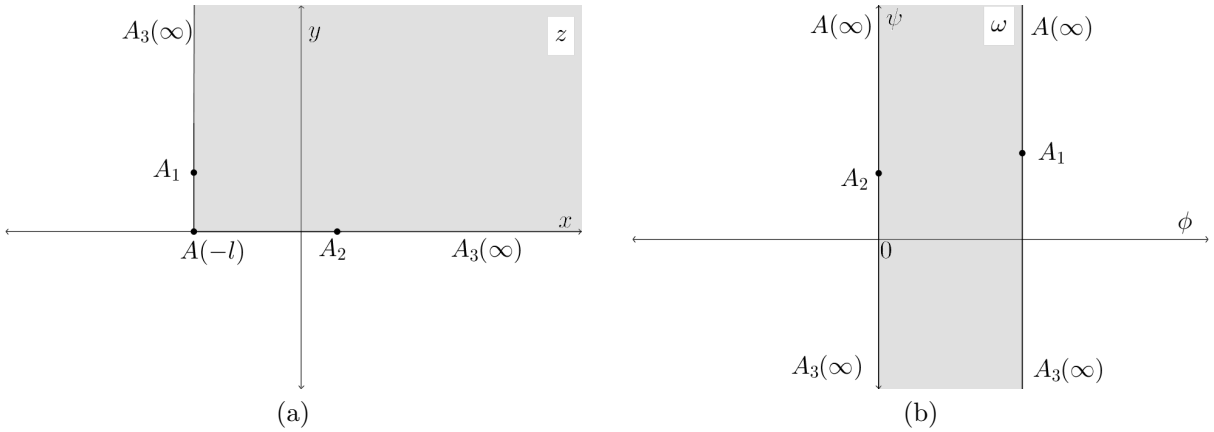

Figure 8: (a) Infinite Extension of Point A (b) Corresponding Complex Potential Plane

The conformal mapping that maps the domain in Figure 8a onto the domain in Figure 8b is given by

$$\omega = M_1(\frac{2}{\pi}\arctan(\frac{y}{x+l}) - \frac{i}{\pi}\ln((x+l)^2+y^2) \tag{66}$$

where M_1 is an arbitrary real number. $\phi(x,y)$ is the real part of ω in Eq. 66. Therefore the general solution of the BVP for the Laplace PDE in the domain in Figure 8a is

$$\phi(x,y) = \frac{2M_1}{\pi}\arctan(\frac{y}{x+l}) \tag{67}$$

On segment A_1A (m from $K5+2$ to $K5+3$),

$x = -l$ and $\frac{\partial \phi}{\partial n} = -\frac{\partial \phi}{\partial x}$

From Eq. 67, one gets,

$\frac{\partial \phi}{\partial n}_{A_1A} = \Omega = -\frac{\partial \phi}{\partial x} = \frac{2M_1}{\pi y}$

At A_1, $y = y_{K5+2}$,

$$\Omega_{K5+2} = \frac{2M_1}{\pi y} \Longrightarrow M_1 = \frac{\pi y_{K5+2} \Omega_{K5+2}}{2} \tag{68}$$

Now,

$$\frac{\partial \phi}{\partial n}_{A_1 A} = \Omega = -\frac{\partial \phi}{\partial x} = \frac{\Omega_{K5+2} y_{K5+2}}{y} \tag{69}$$

Using in Eq. 69 in Eq. 24 one gets,

$$I^{(p)}_{K5+2,K5+3} = B_{p,K5+2} + \Omega_{K5+2} \int_{y_{K5+2}}^{y_{K5+3}} \frac{y_{K5+2}}{y} \ln \sqrt{(y-y_p)^2 + (l+x)^2} dy$$

$$= B_{p,K5+2} + \Omega_{K5+2} I_{11}(y_{K5+2}, y_{K5+3}, y_p, l + x_p) \tag{70}$$

Therefore one gets,

$$a^{(K5+2)}_{p,K5+2} = I_{11}(y_{K5+2}, y_{K5+3}, y_p, l + x_p)$$

to use in the system to improve the BEM solution instead of using what was found in Chapter 3.3 for $m = K5 + 2$ to $m = K5 + 3$. Ω_{K5+3} is chosen to be excluded from the system when improving the BEM solution by Conformal Mapping.

On segment AA_2 (m from 1 to 2),

$y = 0$ and $\frac{\partial \phi}{\partial n} = -\frac{\partial \phi}{\partial y}$

From Eq. 67 one gets,

$$\frac{\partial \phi}{\partial n}_{AA_2} = \Omega = -\frac{\partial \phi}{\partial y} = \frac{-2M_1}{\pi(x+l)} \tag{71}$$

At A_2, $x = x_2$,

$$\Omega_2 = \frac{-2M_1}{\pi(x_2+l)} \Longrightarrow M_1 = \frac{-\pi(x_2+l)}{2} \tag{72}$$

Now,

$$\frac{\partial \phi}{\partial n}_{AA_2} = \Omega = \frac{(x_2+l)}{(x+l)} \Omega_2 \tag{73}$$

Using Eq. 73 in Eq. 24 one gets,

$$I_{1,2}^{(p)} = B_{p,2} - \Omega_2 \int_{x_1}^{x_2} \frac{(x_2+l)}{(x+l)} \cdot \ln\sqrt{(x-x_p)^2+(y_p)^2}dx \tag{74}$$

$$= B_{p,2} + \Omega_2 I_{11}(x_2+1, x_1+l, x_p-l, y_p) \tag{75}$$

Thus one gets,

$$a_{p,2}^{(1)} = I_{11}(x_2+l, x_1+l, x_p-l, y_p) \tag{76}$$

to use in the system to improve the BEM solution instead of using what was found in Chapter 3.3 for $m = 1$ to $m = 2$. Ω_1 is excluded from the system when improving the BEM solution by Conformal Mapping.

Point E

To determine the local behavior of ϕ and $\frac{\partial\phi}{\partial n}$ near point E, the sides from point E in Figure 2 are extended to infinity preserving the given boundary condition valid near point E as shown in Figure 9a. The corresponding complex potential plane for the domain in Figure 9a is given in Figure 9b.

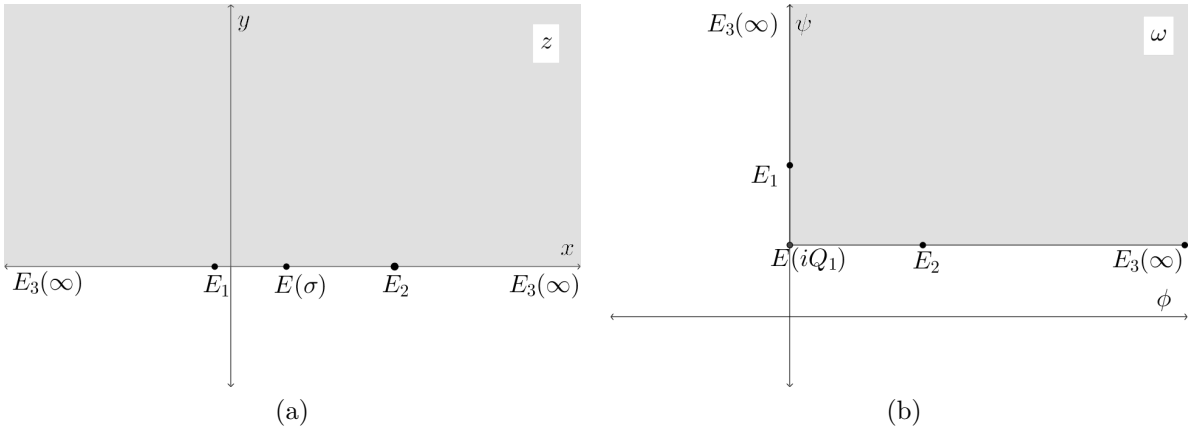

Figure 9: (a) Infinite Extension of Point E (b) Corresponding Complex Potential Plane

The domain Figure 9a is mapped to the domain in Figure 9b by

$$\omega = M_2(z-\sigma)^{\frac{1}{2}} + iQ_1 \tag{77}$$

where M_2 and Q_1 are arbitrary real numbers.

To obtain $\phi(x, y)$ from Eq. 77,

$se^{i\theta} = z - \sigma$

$|s| = |z - \sigma| = \sqrt{(x-\sigma)^2 + y^2}$

for $x > \sigma$, $\theta = \arctan(\frac{y}{x-\sigma})$

for $x < \sigma$, $\theta = \pi + \arctan(\frac{y}{x-\sigma})$

one gets,

$$\phi(x, y) = M_2 s^{\frac{1}{2}} \cos\frac{\theta}{2} \tag{78}$$

as the general solution to the BVP for the Laplace PDE in the domain in Figure 9a.

On E_1E (m from $K1$ to $K1+1$), using the process outlined for point A one obtains,

$$a_{p,K1}^{(K1)} = -I_9(\sigma - x_p, y_p, \sqrt{\sigma - x_{K1}}) \tag{79}$$

to use in the system to improve the BEM solution instead of using what was found in Chapter 3.3 for $m = K1$ to $m = K1+1$.

On E_2E (m from $K1+1$ to $K1+2$), using the process outlined for point A one obtains,

$$a_{p,K1+2}^{(K1+1)} = I_8(x_p - \sigma, y_p, \sqrt{x_{K1+2} - \sigma}) \tag{80}$$

to use in the system to improve the BEM solution instead of what was found in Chapter 3.3 for $m = K1+1$ to $m = K1+2$. Ω_{K1+1} is excluded from the system when improving the BEM solution by Conformal Mapping.

Point C

To determine the local behavior of $\frac{\partial\phi}{\partial n}$ near point C, the sides from point C in Figure 2 are extended to infinity preserving the given boundary condition valid near point C as shown in Figure 10a. The corresponding complex potential plane for the domain in Figure 10a is given in Figure 10b.

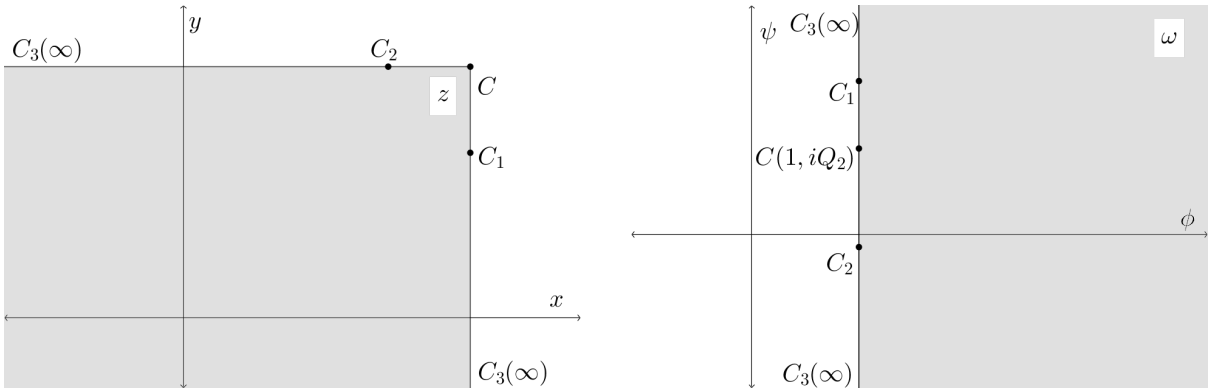

Figure 10: (a) Infinite Extension of Point C (b) Corresponding Complex Potential Plane

The domain Figure 10a is mapped to the domain in Figure 10b by

$$\omega = M_3 \mathrm{e}^{\frac{-i\pi}{2}}(z - l - il)^2 + 1 + iQ_2 \tag{81}$$

where M_3 and Q_2 are arbitrary real numbers.

To obtain $\phi(x, y)$ from Eq. 81,

$se^{i\theta} = z - l - il$

$|s| = |z - l - il| = \sqrt{(x - l)^2 + (y - l)^2}$

$\theta = \arctan(\frac{y-l}{x-l}) + \pi$

one gets,

$$\phi(x, y) = M_3 s^2 \sin 2\theta + 1 \tag{82}$$

as the general solution to the BVP for the Laplace PDE in the in domain in Figure 10a.

On C_1C (m from $K3$ to $K3 + 1$), from Eq. 82 one gets,

$$\frac{\partial \phi}{\partial n} = \frac{\partial \phi}{\partial x} = 2M_3(y - l) \tag{83}$$

Eq. 83 shows the behavior of $\frac{\partial \phi}{\partial n}$ on C_1C is linear, and linear interpolation was used in Chapter 3.3 so no change to $a_{p,K3}^{(K3)}$ in the system is needed.

On CC_2 (m from $K3 + 2$ to $K3 + 2$), from Eq. 82 one gets,

$$\frac{\partial \phi}{\partial n} = \frac{\partial \phi}{\partial y} = 2M_3(x - l) \tag{84}$$

Eq. 84 show the behavior of $\frac{\partial \phi}{\partial n}$ on CC_2 is linear, and linear interpolation was used in Chapter 3.3, so no change to $a_{p,K3+3}^{(K3+2)}$ in the system is needed.

Ω_{K3+1} and Ω_{K3+2} are excluded from the system when improving the BEM solution by Conformal Mapping.

Point D

The extension of the sides from point D is very similar to point C and the boundary conditions valid near point D for the infinite extension are exactly the same as point C. Thus, using what was found from point C, there are no changes to $a_{p,K4+1}^{(K4+1)}$ and $a_{p,K4+4}^{(K4+3)}$. Ω_{K4+2} and Ω_{K4+3} are excluded from the system when improving the BEM solution by Conformal Mapping.

3.6 Results of the Exact Solution, the BEM Solution, and the Improved BEM Solution of Example 1

In this section, the BEM solution of $\phi(x, y)$ and the BEM solution improved by Conformal Mapping of $\phi(x, y)$ are compared to the exact solution of $\phi(x, y)$ to the problem given in Example 1. For the comparison, the following are chosen: $l = 1$, $\sigma = 0.25$, $k_1 = 10$, $k_2 = 70$, $k_3 = 40$, $k_4 = 80$, $k_5 = 40$, and $\epsilon_1 = \epsilon_2 = \epsilon_3 = \epsilon_4 = \epsilon_5 = \epsilon_6 = 0.0001$ (the same were used in Chapter 3.4).

The equipotential lines are shown in Figure 11. The equipotential lines shown are from $\phi(x, y) = 0.1$ to $\phi(x, y) = 0.9$ in increments of 0.1.

From Figure 11, it is clear that the improved BEM solution is closer to the exact solution than the BEM solution without improvement. Figure 12 shows more detail of one in the same equipotential line ($\phi(x, y) = 0.8$) from Figure 11. Table 2 shows some $x-$ values to the corresponding $y-$ values on $\phi(x, y) = 0.8$ from the exact solution and the improved BEM solution. Note that in Mathematica (Wolfram Research, Inc., 2018), the corresponding points on each line must be found manually, which is the reason only

a few corresponding points are given in Table 2.

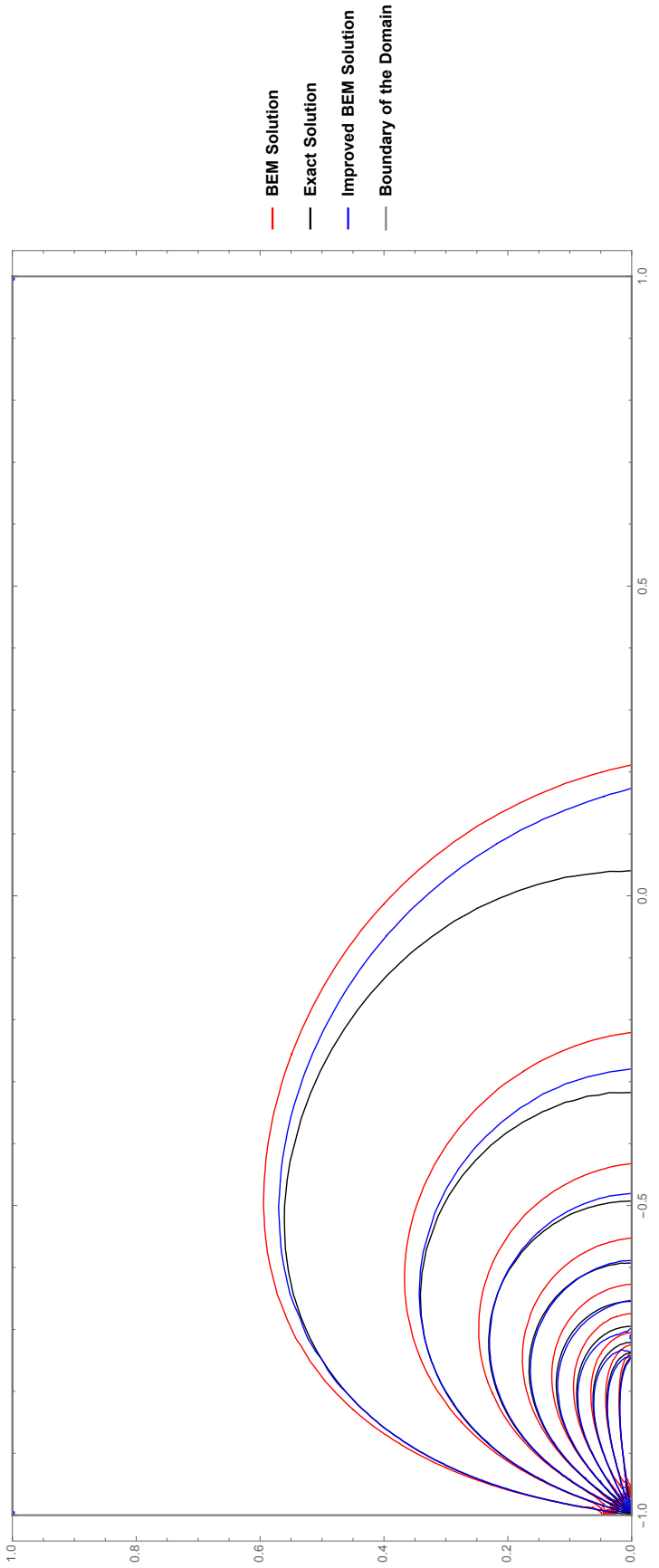

Figure 11: Solution of $\phi(x, y)$ from Example 1 by Conformal Mapping, BEM, and Improved BEM by Conformal Mapping

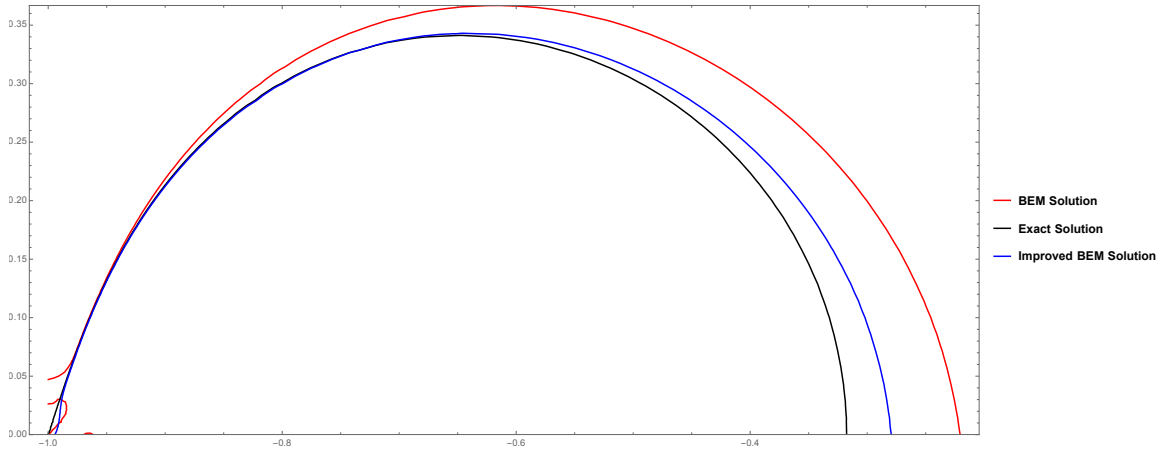

Figure 12: $\phi(x, y) = 0.8$ from the Exact Solution, the BEM Solution, and the Improved BEM Solution

x	y (Exact Solution)	y (BEM Solution Improvement)	Difference of y
-0.3187	0.011	0.1363	0.1253
-0.3218	0.04964	0.1426	0.09296
-0.3252	0.06792	0.1496	0.08168
-0.3284	0.08242	0.1543	0.07188

Table 2: Selected Values on $\phi(x, y) = 0.8$ from the Exact Solution and BEM Solution

Now knowing that the BEM solution of a BVP for two-dimensional Laplace PDE inside a domain with a very singular boundary can be improved by Conformal Mapping, this method can be applied to solving other BVPs for the two-dimensional Laplace PDE in other domains with a very singular boundary.

Chapter 4. Application of Improving the BEM Solution by Conformal Mapping

4.1 Example 2

Example 1 in Chapter 3 was used to demonstrate the need for improvement of the BEM solution for solving a BVP for the two-dimensional Laplace PDE in a domain with a very singular boundary by comparing the BEM solution and the improved BEM solution to the exact solution. In this chapter, another example of solving a BVP for a two-dimensional Laplace PDE in a domain with a singular boundary is shown only this time the exact solution is not known, but the boundary of the domain is more realistic. In a more realistic problem, the flow enters and exits on portions that are not necessarily vertical or horizontal. There is insulation due to man-made objects being inserted in the ground, such as when an important object needs to be kept dry.

Example 2. Solve the BVP for the Laplace PDE with the following boundary conditions:

On AH, $\phi(x,0) = 0, \quad 0 < x < n_1$

On HB, $\frac{\partial \phi}{\partial n}(x,0) = 0, \quad n_1 < x < l_1$

On BC, $\phi(x, x - l_1) = 1, \quad l_1 < x < l_1 + \frac{1}{2}l_2$

On CD, $\phi(x, -x + l_1 + l_2) = 1, \quad l_1 < x < l_1 + \frac{1}{2}l_2$

On DK, $\phi(x, l_2) = 1, \quad n_2 < x < l_1$

On KE, $\frac{\partial \phi}{\partial n}(x, l_2) = 0, \quad 0 < x < n_2$

On EF, $\frac{\partial \phi}{\partial n}(0, y) = 0, \quad \frac{l_2}{2} < y < l_2$

On FG, $\frac{\partial \phi}{\partial n}(x, -x + \frac{l_2}{2}) = 0, \quad 0 < x < \frac{l_2}{4}$

On GA, $\frac{\partial \phi}{\partial n}(x, x) = 0, \quad 0 < x < \frac{l_2}{4}$

where $0 < n_1 < l_1$ and $0 < n_2 < 0$. When solving the problem using BEM, the values of l_1, l_2, n_1, and n_2 are chosen. The physical domain of the problem is shown in Figure 13.

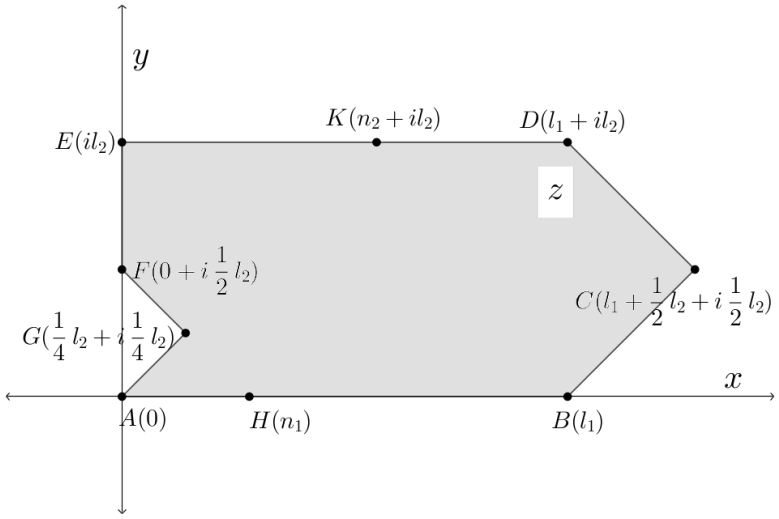

Figure 13: Physical Domain of Example 2

Points A, B, C, D, E, F, G, H, and K are singular points. At point A, an insulated portion and free exit meet at an angle of $\frac{\pi}{4}$. At point H, the free exit and an insulated portion meet at an angle of π. At point B, an insulated portion and free entrance meet at angle $\frac{3\pi}{4}$. At point C, one in the same potential meet at an angle of $\frac{\pi}{2}$. At point D, one in the same potential meet at $\frac{3\pi}{4}$ At point K, the free entrance and an insulated portion meet at angle π. At point E, insulated portions meet at angle $\frac{\pi}{2}$. At point F, insulated portions meet at $\frac{3\pi}{4}$. Lastly, at point G, insulated portions meet at $\frac{3\pi}{2}$.

4.2 BEM Solution of Example 2

The boundary of the domain in Figure 13 is discretized as follows: AH is discretized into k_1 elements, HB is discretized into k_2 elements, BC is discretized into k_3 elements, CD is discretized into k_4 elements, DK is discretized into k_5 elements, KE is discretized into k_6 elements, EF is discretized into k_7 elements, FG is discretized into k_8 elements, and lastly GA is discretized into k_9 elements. Instead of having a node at each point A, B, C, and D, two nodes approach each point. Through experimentation, it was discovered that there is no need to use two nodes that approach each point E, F, G, H, and K instead of using a node at each of those points. Thus, total number of nodes is $N = k_1 + k_2 + k_3 + k_4 + k_5 + k_6 + k_7 + k_8 + k_9 + 4$, and the choice of the numbering of the nodes begins at the first node after point A. For notation,

$K1 = k_1, K2 = k_1 + k_2, ..., K9 = k_1 + k_2 + k_3 + k_4 + k_5 + k_6 + k_7 + k_8 + k_9$.

The integrals from Eq. 24 are developed in this section. Then, what is needed to solve the system in Eq. 31 is found by using Eq. 28 and Eq. 29. All the integrals that come from Eq. 24 on each portion of the boundary are defined and solved in Appendix A. Additionally, details of finding the BEM solution were given in Chapter 3.3. In this section, only the information needed for Eq. 24 and the result of evaluating Eq. 24 on each portion of the boundary of the domain in Figure 13 are given.

On the portion of the boundary AH,

$y = 0$ and $\epsilon_1 < x < n_1$, where ϵ_1 is the distance after point A.

$\phi(x, 0) = 0$

$\frac{\partial \phi}{\partial n}(x, 0) = \Omega_m \frac{x_{m+1} - x}{x_{m+1} - x_m} + \Omega_{m+1} \frac{x - x_m}{x_{m+1} + x_m}$

$r_p = \sqrt{(x - x_p)^2 + y_p^2}$

From Eq. 24 one gets,

$$a_{p,m}^{(m)} = -I_1(x_m, x_{m+1}, x_p, y_p) \tag{85}$$

for two nodes, m to $m+1$ on AH. $a_{p,m}^{(m-1)}$ is found from Eq. 33. There is no contribution to B_p on AH.

On the portion of the boundary HB,

$y = 0$ and $n_1 < x < l_1 - \epsilon_2$, where ϵ_2 is the distance before point B.

$\frac{\partial \phi}{\partial n}(x, 0) = 0$

$\phi(x, 0) = \Omega_m \frac{x_{m+1} - x}{x_{m+1} - x_m} + \Omega_{m+1} \frac{x - x_m}{x_{m+1} - x_m}$

$r_p = \sqrt{(x - x_p)^2 + y_p^2}$

From Eq. 24 one gets,

$$a_{p,m}^{(m)} = I_2(x_m, x_{m+1}, x_p, y_p) \tag{86}$$

for two nodes, m to $m+1$ on HB. $a_{p,m}^{(m-1)}$ is found from Eq. 33. There is no contribution

to B_p on HB.

On the portion of the boundary BC,

$y = x - l_1$ and $l_1 + \frac{1}{\sqrt{2}}\epsilon_3 < x < l_1 + \frac{1}{2}l_2 - \frac{1}{\sqrt{2}}\epsilon_4$ where ϵ_3 is the distance after B and ϵ_4 is the distance before point C.

$\phi(x, x - l_1) = 1$

$\frac{\partial\phi}{\partial n}(x, y) = \Omega_m \frac{x_{m+1}-x}{x_{m+1}-x_m} + \Omega_{m+1}\frac{x-x_m}{x_{m+1}+x_m}$

$r_p = \sqrt{(x - x_p)^2 + (y - y_p)^2} = \sqrt{(x - x_p)^2 + (x - l_1 - y_p)^2} =$

$\sqrt{2(x - (x_p + \frac{1}{2}(l_1 + y_p - x_p)))^2 + \frac{1}{2}(l_1 + y_p - x_p)^2} =$

$\sqrt{2}\sqrt{(x - (x_p + \frac{1}{2}(l_1 + y_p - x_p)))^2 + (\frac{l_1+y_p-x_p}{2})^2}$

$\frac{\partial r_p}{\partial n}(x, y) = \frac{1}{r_p\sqrt{2}}(x - x_p - y + y_p) = \frac{1}{2}\frac{x-x_p-x+l_1+y_p}{\sqrt{(x-(x_p+\frac{1}{2}(l_1+y_p-x_p)))^2+(\frac{l_1+y_p-x_p}{2})^2}} =$

$\frac{1}{2}\frac{l_1+y_p-x_p}{\sqrt{(x-(x_p+\frac{1}{2}(l_1+y_p-x_p)))^2+(\frac{l_1+y_p-x_p}{2})^2}}$

From Eq. 24 one gets,

$$a_{p,m}^{(m)} = -\sqrt{2}I_1(x_m, x_{m+1}, x_p + \frac{1}{2}(l_1 + y_p - x_p), |\frac{1}{2}(l_1 + y_p + x_p)| - \frac{1}{4}\ln 2(x_{m+1} - x_m) \quad (87)$$

for two nodes, m to $m + 1$ on BC. $a_{p,m}^{(m-1)}$ is found from Eq. 33. Since $\phi(x, y)$ is known on BC from Eq. 24 one gets,

$$B_{p,m} = I_3(x_m, x_{m+1}, x_p + \frac{1}{2}(l_1 + y_p - x_p), \frac{1}{2}(l_1 + y_p + x_p)) \quad (88)$$

On the portion of the boundary CD,

$y = -x + l_1 + l_2$ and $l_1 + \frac{1}{2}l_2 - \frac{1}{\sqrt{2}}\epsilon_5 < x < l_1 + \frac{1}{\sqrt{2}}\epsilon_6$ where ϵ_5 is the distance after point C and ϵ_6 is the distance before point D.

$\phi(x, -x + l_1 + l_2) = 1$

$\frac{\partial\phi}{\partial n}(x, -x + l_1 + l_2) = \Omega_m \frac{x_{m+1}-x}{x_{m+1}-x_m} + \Omega_{m+1}\frac{x-x_m}{x_{m+1}+x_m}$

$r_p = \sqrt{(x - x_p)^2 + (y - y_p)^2} = \sqrt{(x - x_p)^2 + (-x + l_1 + l_2 - y_p)^2} =$

$\sqrt{(x - x_p)^2 + (x - l_1 - l_2 + y_p)^2} =$

$\sqrt{2(x-(x_p+\frac{1}{2}(l_1+l_2-y_p-x_p)))^2+\frac{1}{2}(l_1+l_2-y_p-x_p)^2}=$

$\sqrt{2}\sqrt{((x-(x_p+\frac{1}{2}(l_1+l_2-y_p-x_p)))^2+(\frac{l_1+l_2-y_p-x_p}{2})^2}$

$\frac{\partial r_p}{\partial n}(x,y)=\frac{1}{\sqrt{2}}\frac{x-x_p+y-y_p}{r_p}=\frac{1}{r_p\sqrt{2}}(x-x_p+-x+l_1+l_2-y_p)=\frac{1}{r_p\sqrt{2}}(l_1+l_2-x_p-y_p)=$

$\frac{1}{2}\frac{(l_1+l_2-x_p-y_p)}{\sqrt{((x-(x_p+\frac{1}{2}(l_1+l_2-y_p-x_p)))^2+(\frac{l_1+l_2-y_p-x_p}{2})^2}}$

From Eq. 24 one gets,

$$a_{p,m}^{(m)}=\sqrt{2}I_1(x_m,x_{m+1},x_p+\frac{1}{2}(l_1+l_2-y_p-x_p),\frac{1}{2}|(l_1+l_2-y_p-x_p)|+\frac{1}{4}\ln 2(x_{m+1}-x_m) \quad (89)$$

for two nodes, m to $m+1$ on CD. $a_{p,m}^{(m-1)}$ is found from Eq. 33. Since $\phi(x,-x+l_1+l_2)=1$ on CD, from Eq. 24,

$$B_{p,m}=-I_3(x_m,x_{m+1},x_p+\frac{1}{2}(l_1+l_2-y_p-x_p),\frac{1}{2}(l_1+l_2-y_p-x_p)) \quad (90)$$

On the portion of the boundary DK,

$y=l_2$ and $n_2<x<l_1-\epsilon_7$ where ϵ_7 is the distance after point D.

$\phi(x,l_2)=1$

$\frac{\partial\phi}{\partial n}(x,y)=\Omega_m\frac{x_{m+1}-x}{x_{m+1}-x_m}+\Omega_{m+1}\frac{x-x_m}{x_{m+1}+x_m}$

$r_p=\sqrt{(x-x_p)^2+(l_2-y_p)^2}$

$\frac{\partial r_p}{\partial n}=\frac{l_2-y_p}{\sqrt{(x-x_p)^2+(l_2-y_p)^2}}$

From Eq. 24 one gets,

$$a_{p,m}^{(m)}=I_1(x_m,x_{m+1},x_p,l_2-y_p) \quad (91)$$

for two nodes, m to $m+1$ on DK. $a_{p,m}^{(m-1)}$ is found from Eq. 33. Since $\phi(x,l_2)=1$ on DK, From Eq. 24 one gets,

$$B_{p,m}=-I_3(x_m,x_{m+1},x_p,l_2-y_p) \quad (92)$$

On the portion of the boundary KE,

$y = l_2$ and $0 < x < n_2$

$\phi(n_2, l_2) = 1$

$\phi(x, l_2) = \Omega_m \frac{x_{m+1}-x}{x_{m+1}-x_m} + \Omega_{m+1} \frac{x-x_m}{x_{m+1}+x_m}$

$\frac{\partial \phi}{\partial n}(x, l_2) = 0$

$r_p = \sqrt{(x-x_p)^2 + (l_2-y_p)^2}$

$\frac{\partial r_p}{\partial n}(x, l_2) = \frac{l_2-y_p}{\sqrt{(x-x_p)^2+(l_2-y_p)^2}}$

From Eq. 24 one gets,

$$a_{p,m}^{(m)} = -I_2(x_m, x_{m+1}x_p, l_2 - y_p) \tag{93}$$

for two nodes, m to $m+1$ on KE. $a_{p,m}^{(m-1)}$ is found from Eq. 33. Using Eq. 33 one can find $a_{p,m}^{(m-1)}$. Since $\phi(n_2, l_2) = 1$, from Eq. 24

$$B_{p,K5+4} = -I_2(x_{_{K5+4}}, x_{_{K5+5}}, x_p, l_2 - y_p) \tag{94}$$

On the portion of the boundary EF,

$x = 0$ and $\frac{1}{2}l_2 < y < l_2$

$\phi(0, y) = \Omega_m \frac{y_{m+1}-y}{y_{m+1}-y_m} + \Omega_{m+1} \frac{y-y_m}{y_{m+1}+y_m}$

$\frac{\partial \phi}{\partial n}(0, y) = 0$

$r_p = \sqrt{(y-y_p)^2 + x_p^2}$

$\frac{\partial r_p}{\partial n}(0, y) = \frac{x_p}{(y-y_p)^2+x_p^2}$

From Eq. 24 one gets,

$$a_{p,m}^{(m)} = -I_2(y_m, y_{m+1}, y_p, x_p) \tag{95}$$

for two nodes, m to $m+1$ on EF. $a_{p,m}^{(m-1)}$ is found from Eq. 33. There is no contribution to B_p on EF.

On the portion of the boundary FG,

$y = -x + \frac{1}{2}l_2$ and $0 < x < \frac{1}{4}l_2$

$\phi(x, -x + \frac{1}{2}l_2) = \Omega_m \frac{x_{m+1}-x}{x_{m+1}-x_m} + \Omega_{m+1} \frac{x-x_m}{x_{m+1}+x_m}$

$\frac{\partial \phi}{\partial n}(x, -x + \frac{1}{2}l_2) = 0$

$r_p = \sqrt{(x-x_p)^2 + (-x+l_2-y_p)^2} = \sqrt{2(x - \frac{1}{2}(x_p - y_p + \frac{1}{2}l_2))^2 + \frac{1}{2}(x_p + y_p - \frac{l_2}{2})^2} =$

$\sqrt{2}\sqrt{(x - \frac{1}{2}(x_p - y_p + \frac{1}{2}l_2))^2 + (\frac{x_p+y_p-\frac{l_2}{2}}{2})^2}$

$\frac{\partial r_p}{\partial n}(x, -x+\frac{1}{2}l_2) = \frac{-1}{r_p\sqrt{2}}(\frac{l_2}{2} - x_p - y_p) = \frac{1}{r_p\sqrt{2}}(x_p + y_p - \frac{l_2}{2}) = \frac{1}{2}\frac{x_p+y_p-\frac{l_2}{2}}{\sqrt{(x-\frac{1}{2}(x_p-y_p+\frac{1}{2}l_2))^2 - (\frac{x_p+y_p-\frac{l_2}{2}}{2})^2}}$

From Eq. 24 one gets,

$$a_{p,m}^{(m)} = I_2(x_m, x_{m+1}, \frac{1}{2}(x_p - y_p + \frac{l_2}{2}), \frac{1}{2}(x_p + y_p - \frac{l_2}{2})) \tag{96}$$

for two nodes, m to $m+1$ on FG. $a_{p,m}^{(m-1)}$ is found from Eq. 33. There is no contribution to B_p on FG.

On the portion of the boundary GA,

$y = x$ and $\frac{1}{\sqrt{2}}\epsilon_8 < x < \frac{1}{4}l_2$ where ϵ_8 is the distance before point A.

$\phi(x, x) = \Omega_m \frac{x_{m+1}-x}{x_{m+1}-x_m} + \Omega_{m+1} \frac{x-x_m}{x_{m+1}+x_m}$

$\frac{\partial \phi}{\partial n}(x, x) = 0$

$r_p = \sqrt{(x-x_p)^2 + (x-y_p)^2} = \sqrt{2(x - \frac{1}{2}(x_p + y_p))^2 + \frac{1}{2}(x_p - y_p)^2} =$

$\sqrt{2}\sqrt{(x - \frac{1}{2}(x_p + y_p))^2 + (\frac{x_p-y_p}{2})^2}$

$\frac{\partial r_p}{\partial n}(x, x) = \frac{1}{r_p\sqrt{2}}(-x + x_p + y - y_p) = \frac{1}{r_p\sqrt{2}}(x_p - y_p) = \frac{1}{2}\frac{x_p+y_p-\frac{l_2}{2}}{\sqrt{(x-\frac{1}{2}(x_p+y_p))^2 - (\frac{x_p-y_p}{2})^2}}$

From Eq. 24 one gets,

$$a_{p,m}^{(m)} = -I_2(x_m, x_{m+1}, \frac{1}{2}(x_p + y_p), \frac{1}{2}(x_p - y_p)) \tag{97}$$

for two nodes, m to $m+1$ on GA. $a_{p,m}^{(m-1)}$ is found from Eq. 33. There is no contribution to B_p on GA.

Thus, everything has been found in order to find the coefficient $A_{p,m}$ and B_p for m and p from 1 to N in order to solve the system in Eq. 31. Then, using the results of the system in Eq. 31 in Eq. 34, the solution of $\phi(x, y)$ of Example 2 is found.

4.3 Conformal Mapping Improvement of the BEM Solution in Example 2

An overview of using Conformal Mapping to improve the BEM solution was provided in Chapter 1.2. In Chapter 3.5, the details of how to find the exact Conformal Mapping solution near a singular point and how to use that solution in Eq. 24 to improve the BEM solution were shown for point singular A in Example 1. In this section, the method outlined in Chapter 1.2 and Chapter 3.5 is used for singular points A, B, C, D, E, F, G, H, and K.

Point A

To determine the local behavior of ϕ and $\frac{\partial \phi}{\partial n}$ near point A, the sides from point A in Figure 13 are extended to infinity preserving the given boundary condition valid near point A. The behavior of the exact solution in the infinite domain is found by Conformal Mapping and is imposed for the unknown variable in Eq. 24 on the elements adjacent to point A. The improvements to use in the system in Eq. 31 are:

$$a_{p,K9+3}^{(K9+3)} = \frac{1}{x_{K9+3}} I_{10}(x_1, x_{K9+3}, \frac{1}{2}(x_p + y_p), \frac{1}{2}(x_p - y_p)) \tag{98}$$

$$a_{p,2}^{(1)} = -I_{13}(x_p, y_p, x_2) \tag{99}$$

and Ω_{K9+4} and Ω_1 are excluded from the system.

Point H

To determine the local behavior of ϕ and $\frac{\partial \phi}{\partial n}$ near point H, the sides from point H in Figure 13 are extended to infinity preserving the given boundary condition valid near point H. The behavior of the exact solution in the infinite domain is found by Conformal Mapping and is imposed for the unknown variable in Eq. 24 on the elements adjacent to point H. The improvements to use in the system in Eq. 31 are:

$$a_{p,K1}^{(K1)} = I_9(n_1 - x_p, y_p, \sqrt{n_1 - x_{K1}}) \tag{100}$$

$$a_{p,K1+2}^{(K1)} = I_8(x_p - n_1, y_p, \sqrt{x_{K1+2} - n_1}) \tag{101}$$

and Ω_{K1+1} is excluded from the system.

Point B

To determine the local behavior of ϕ and $\frac{\partial \phi}{\partial n}$ near point B, the sides from point B in Figure 13 are extended to infinity preserving the given boundary condition valid near point B. The behavior of the exact solution in the infinite domain is found by Conformal Mapping and is imposed for the unknown variable in Eq. 24 on the elements adjacent to point B. The improvements to use in the system in Eq. 31 are:

$$a_{p,K2}^{(K2)} = I_{12}(l_1 - x_p, y_p, \sqrt[3]{l_1 - x_{K2}}) \tag{102}$$

$$B_{p,K2} = -I_{12}(l_1 - x_p, y_p, \sqrt[3]{l_1 - x_{K2}}) + I_3(x_{K2}, x_{K2+1}, x_p, y_p) \tag{103}$$

$$a_{p,K2+3}^{(K2+2)} = \frac{-3\sqrt{2}}{4}\ln 2(x_{K2+3} - l_1) - \frac{3\sqrt{2}}{2} I_4(\frac{1}{2}(x_p - l_1 + y_p), |\frac{1}{2}(l_1 - x_p + y_p)|, \sqrt[3]{x_{K2+3} - l_1}) \tag{104}$$

and Ω_{K2+1} and Ω_{K2+2} are excluded from the system.

Point C

To determine the local behavior of $\frac{\partial \phi}{\partial n}$ near point C, the sides from point C in Figure 13 are extended to infinity preserving the given boundary condition valid near point C. The behavior of the exact solution in the infinite domain is found by Conformal Mapping. Similar to points C and D in Chapter 3.5, there is no alternation needed because the behavior the normal derivative near C is linear, and linear interpolation was used to approximate $\frac{\partial \phi}{\partial n}$ on the elements adjacent to point C. Ω_{K3+2} and Ω_{K3+3} are excluded from the system.

Point D

To determine the local behavior of $\frac{\partial \phi}{\partial n}$ near point D, the sides from point D in Figure 13 are extended to infinity preserving the given boundary condition valid near point D. The behavior of the exact solution in the infinite domain is found by Conformal Mapping and is imposed for the unknown variable in Eq. 24 on the elements adjacent to point D. The improvements to use in the system in Eq. 31 are:

$$a_{p,K4+2}^{(K4+2)} = -\frac{3\sqrt{2}}{8}\ln 2(x_{K4+2}-l_1)-\sqrt{2}I_6(\frac{1}{2}(x_p-l_1-y_p+l_2), |\frac{1}{2}(x_p+y_p-l_1-l_2)|, \sqrt[3]{x_{K4+2}-l_1}) \tag{105}$$

$$a_{p,K4+5}^{(K4+4)} = I_6(l_1-x_p, l_2-y_p, \sqrt[3]{l_1-x_{K4+5}}) \tag{106}$$

and Ω_{K4+3} and Ω_{K4+4} are excluded from the system.

Point K

To determine the local behavior of ϕ and $\frac{\partial \phi}{\partial n}$ near point K, the sides from point K in Figure 13 are extended to infinity preserving the given boundary condition valid near point K. The behavior of the exact solution in the infinite domain is found by Conformal Mapping and is imposed for the unknown variable in Eq. 24 on the elements adjacent to point K. The improvements to use in the system in Eq. 31 are:

$$a_{p,K5+3}^{(K5+3)} = -I_9(x_p-n_2, l_2-y_p, \sqrt{x_{K5+3}-n_2}) \tag{107}$$

$$a_{p,K5+5}^{(K5+4)} = I_8(n_2-x_p, l_2-y_p, \sqrt{n_2-x_{K5+5}}) \tag{108}$$

$$B_{p,K5+4} = -I_8(n_2-x_p, l_2-y_p, \sqrt{n_2-x_{K5+5}}) - I_3(n_2, x_{K5+5}, x_p, l_2-y_p) \tag{109}$$

and Ω_{K5+4} is excluded from the system.

Point E

To determine the local behavior of ϕ near point E, the sides from point E in Figure 13 are extended to infinity preserving the given boundary condition valid near point E. The behavior of the exact solution in the infinite domain is found by Conformal Mapping and is imposed for the unknown variable in Eq. 24 on the elements adjacent to point E. The improvements to use in the system in Eq. 31 are:

$$a_{p,K6+3}^{(K6+3)} = \frac{1}{x_{K6+3}} I_{10}(x_p, l_2 - y_p, x_{K6+3}) \tag{110}$$

$$a_{p,K6+4}^{(K6+3)} = I_3(x_{K6+4}, x_{K6+3}, x_p l_2 - y_p) - \frac{1}{x_{K6+3}} I_{10}(x_p, l_2 - y_p, x_{K6+3}) \tag{111}$$

$$a_{p,K6+4}^{(K6+4)} = -I_3(y_{K6+4}, y_{K6+5}, y_p, x_p) - \frac{1}{l_2 - y_{K6+5}} I_{10}(l_2 - y_p, x_p, l_2 - y_{K6+5}) \tag{112}$$

$$a_{p,K6+5}^{(K6+4)} = \frac{1}{l_2 - y_{K6+5}} I_{10}(l_2 - y_p, x_p, l_2 - y_{K6+5}) \tag{113}$$

Point F

To determine the local behavior of ϕ near point F, the sides from point F in Figure 13 are extended to infinity preserving the given boundary condition valid near point F. The behavior of the exact solution in the infinite domain is found by Conformal Mapping and is imposed for the unknown variable in Eq. 24 on the elements adjacent to point F. The improvements to use in the system in Eq. 31 are:

$$a_{p,K7+3}^{(K7+3)} = I_5(y_p - \frac{1}{2} l_2, x_p, \sqrt[3]{y_{K7+3} - \frac{1}{2} l_2}) \tag{114}$$

$$a_{p,K7+4}^{(K7+3)} = -I_5(y_p - \frac{1}{2}l_2, x_p, \sqrt[3]{y_{K7+3} - \frac{1}{2}l_2}) - I_3(y_{K7+2}, y_{K7+3}, y_p, x_p) \tag{115}$$

$$a_{p,K7+4}^{(K7+4)} = -I_5(\frac{1}{2}(x_p + \frac{1}{2}l_2 - y_p), \frac{1}{2}(x_p + y_p - \frac{1}{2}l_2), \sqrt[3]{x_{K7+5}}) +$$

$$I_3(y_{K7+4}, y_{K7+5}, \frac{1}{2}(x_p + \frac{1}{2}l_2 - y_p), \frac{1}{2}(x_p, y_p, \frac{1}{2}l_2)) \tag{116}$$

$$a_{p,K7+5}^{(K7+4)} = I_5(\frac{1}{2}(x_p + \frac{1}{2}l_2 - y_p), \frac{1}{2}(x_p + y_p - \frac{1}{2}l_2), \sqrt[3]{x_{K7+5}}) \tag{117}$$

Point G

To determine the local behavior of ϕ near point G, the sides from point G in Figure 13 are extended to infinity preserving the given boundary condition valid near point G. The behavior of the exact solution in the infinite domain is found by Conformal Mapping and is imposed for the unknown variable in Eq. 24 on the elements adjacent to point G. The improvements to use in the system in Eq. 31 are:

$$a_{p,K8+3}^{(K8+3)} = I_{12}(\frac{1}{4}l_2 - \frac{1}{2}(x_p - y_p + \frac{1}{2}l_2), \frac{1}{2}(x_p + y_p - \frac{1}{2}l_2), \sqrt[3]{\frac{1}{4}l_2 - x_{K8+3}}) \tag{118}$$

$$a_{p,K8+4}^{(K8+3)} = -I_{12}(\frac{1}{4}l_2 - \frac{1}{2}(x_p - y_p + \frac{1}{2}l_2), \frac{1}{2}(x_p + y_p - \frac{1}{2}l_2), \sqrt[3]{\frac{1}{4}l_2 - x_{K8+3}}) +$$

$$I_3(x_{K8+3}, x_{K8+4}, \frac{1}{2}(x_p - y_p + \frac{1}{2}l_2), \frac{1}{2}(x_p + y_p - \frac{1}{2}l_2)) \tag{119}$$

$$a_{p,K8+4}^{(K8+4)} = -I_{12}(\frac{1}{4}l_2 - \frac{1}{2}(x_p + y_p), \frac{1}{2}(x_p - y_p), \sqrt[3]{\frac{1}{4}l_2 - x_{K8+5}}) -$$

$$I_3(x_{K8+4}, x_{K8+5}, \frac{1}{2}(x_p + y_p), \frac{1}{2}(x_p - y_p)) \tag{120}$$

$$a_{p,K8+5}^{(K8+4)} = I_{12}(\frac{1}{4}l_2 - \frac{1}{2}(x_p + y_p), \frac{1}{2}(x_p - y_p), \sqrt[3]{\frac{1}{4}l_2 - x_{K8+5}}) \tag{121}$$

Eqs. 98-121 are used to improve the coefficients of the unknown values, $A_{p,m}$, and the evaluation of the known values, $B_{p,m}$, found in Chapter 4.2. The new system is solved by using Eq. 31, and then Eq. 34 is used to solve for $\phi(x, y)$ in Example 2. Some results are given in Chapter 4.4

4.4 Results of the BEM and Improved BEM Solution of Example 2

In this section, the BEM solution of $\phi(x, y)$ and the BEM solution improved by Conformal Mapping of $\phi(x, y)$ to the problem given in Example 2 will be compared. For the comparison, the following are chosen: $l_1 = 4$, $l_2 = 2$, $n_1 = 1$, $n_2 = 1$, $k_1 = 25$, $k_2 = 75$, $k_3 = 35$, $k_4 = 35$, $k_5 = 75$, $k_6 = 25$, $k_7 = 25$, $k_8 = 18$, $k_9 = 18$ and $\epsilon_1 = \epsilon_2 = \epsilon_3 = \epsilon_4 = \epsilon_5 = \epsilon_6 = \epsilon_7 = \epsilon_8 = 0.0001$.

The equipotential lines, which solve the BVP in Example 2, are shown in Figure 14. The equipotential lines shown are from $\phi(x, y) = 0.1$ to $\phi(x, y) = 0.9$ in increments of 0.1.

Figure 15 shows more detail of one in the same equipotential line ($\phi(x, y) = 0.6$) from Figure 14. Table 3 shows some $x-$values to the corresponding $y-$values on $\phi(x, y) = 0.6$ from BEM Solution and the improved BEM solution. Note that in Mathematica (Wolfram Research, Inc., 2018), the corresponding points on each line must be found manually, which is the reason only a few corresponding points are given in Table 3.

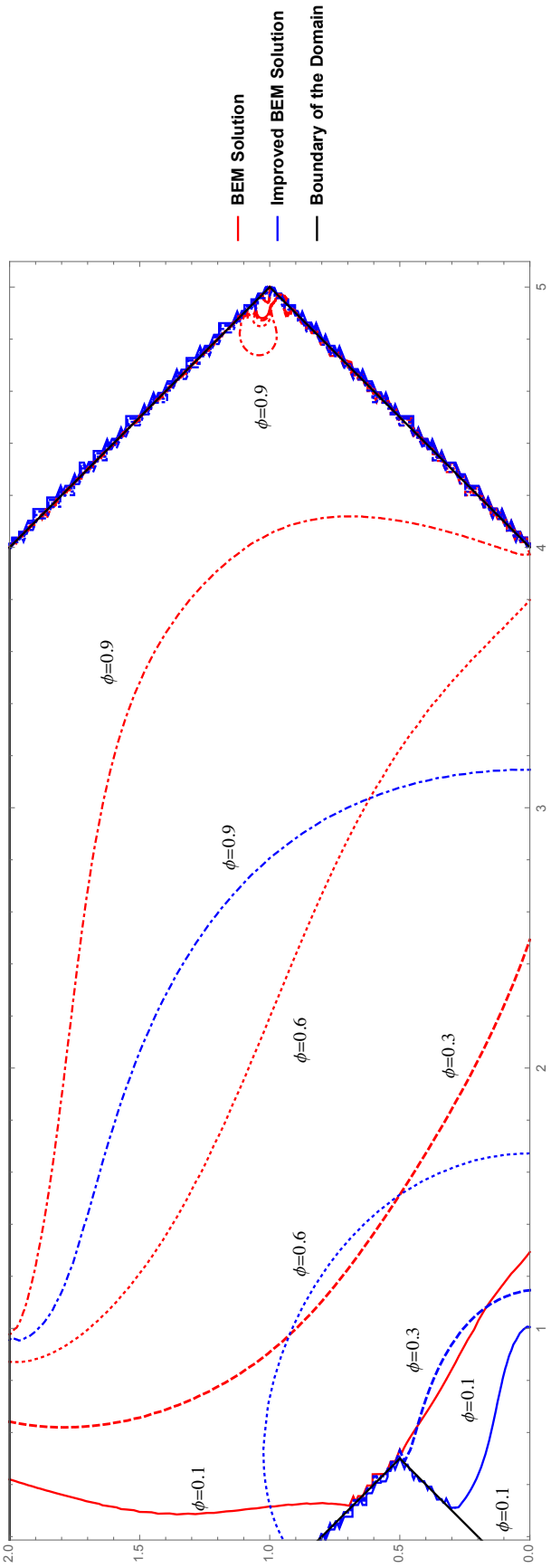

Figure 14: BEM Solution and Improved BEM Solution of Example 2

We know from Example 1 that the BEM solution of $\phi(x, y)$ in a domain with a very singular boundary is improved by Conformal Mapping. We are also able to observe the behavior of the BEM solution and improved BEM solution by Conformal Mapping. First, the BEM solution does not approach HB at an angle of $\frac{\pi}{2}$ as expected from the explanation of the flow net in Chapter 2.2. On the other hand, for the improved BEM solution, it can be observed that the flow net appears as one would expect which is the equipotential lines approach the portions of the boundary where $\frac{\partial \phi}{\partial n} = 0$ at an angle of $\frac{\pi}{2}$.

There are a couple of ways to determine the accuracy of the improved BEM solution. The first is by using functional analysis, which is not done in this thesis. The second is to compare the numerical solution to the exact solution. Although the exact solution to Example 2 was not found, we did impose the behavior of exact solution when improving BEM, which means there is some comparison with the exact solution when observing the improved BEM solution of Example 2. Additional conclusions from observing the behavior of the equipotentials lines for Example 1 and Example 2 are given in Chapter 5.

Chapter 5. Conclusions

In this thesis, two examples of improving the BEM solution to the potential (modeled by the two-dimensional Laplace PDE) of underground water flow in a domain with a very singular boundary were given in Chapters 3 and 4. From our observations of these two examples, it has been shown that the BEM solution of a BVP for the two-dimensional Laplace PDE inside a domain with a very singular boundary needs improvement. By using the hands on method from Muleshkov (1988), we are able to compare the behavior of the BEM solution to the behavior of the exact solution found by Conformal Mapping.

In Example 1, since we know the exact solution, we can compare it to the BEM solution which shows the needs for improvement of the BEM solution. We are able to know what kind of improvement is needed by comparing the BEM solution improved by Conformal Mapping to the exact solution also found by Conformal Mapping. This demonstrates the method of improving the BEM solution by Conformal Mapping can be applied to other domains with a very singular boundary. On the other hand, in Example 2, we do not have the exact solution to compare with each method (BEM and improved BEM by Conformal Mapping), but we do know from Example 1 that by imposing the behavior of the exact solution adjacent to singular points in BEM the BEM solution is improved.

Some additional observations were made through experimentation that are noteworthy to mention. From our observations, when the singularities are farther away from each other, BEM seems to be a useful tool to solve BVPs for the two-dimensional Laplace PDE in the given domain with a very singular boundary. However, when the singularities are closer together, from observation it appears that the BEM solution needs to be improved. Conformal Mapping to find the local behavior of the unknown variable (ϕ or $\frac{\partial \phi}{\partial n}$) on the elements adjacent to singularities is a powerful tool because it is hands on and allows for one to use the behavior of the exact solution rather than guessing to use quadratic, cubic, or any other arbitrarily chosen interpolation.

Another observation, from experimenting, was that when using BEM, approximately equal length elements on every portion of the boundary should be used. However, from

observation by experimentation, this is not the case for the improved BEM solution by Conformal Mapping i.e. the same number of elements could be used on each portion even if the length of the elements are not the same. To demonstrate this, Figure 15 shows the family of equipotentials lines found by BEM and improved BEM by Conformal Mapping. The following are chosen: $l_1 = 4$, $l_2 = 2$, $n_1 = 1$, $n_2 = 1$, $k_1 = k_2 = k_3 = k_4 = k_5 = k_6 = k_7 = k_8 = k_9 = 50$, and $\epsilon_1 = \epsilon_2 = \epsilon_3 = \epsilon_4 = \epsilon_5 = \epsilon_6 = \epsilon_7 = \epsilon_8 = 0.0001$ so that there are the same number of elements on every portion of the boundary, and some of the elements are only a few times bigger than others. Comparing the family of equipotentials lines in Figure 14 with the family of equipotential lines in Figure 15, it is clear that unequal length elements could be used for the method of improving the BEM solution by Conformal Mapping.

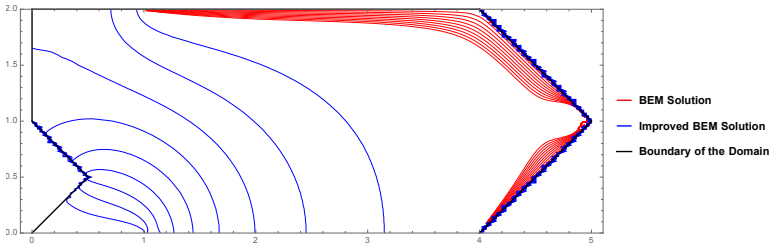

(a)

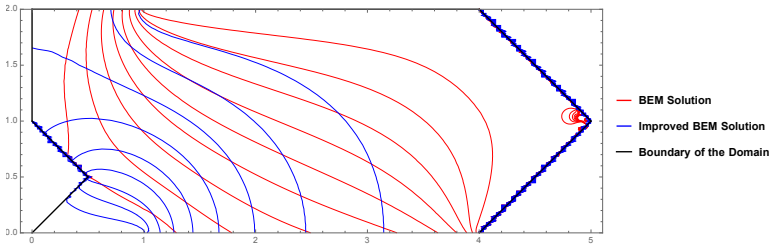

(b)

Figure 15: (a) Unequal Length Elements for the BEM Solution and Improved BEM Solution of Example 2 (b) Approximately Equal Length Elements for the BEM Solution and Improved BEM Solution of Example 2

In this thesis, the method of improving the BEM solution by Conformal Mapping from Muleshkov (1988) was used for two-dimensional confined flow with straight line segments for each portion of the boundary. In the future, one could try to use this method when arcs of circles are portions of the boundary. In addition, one could try to use this method for two-dimensional unconfined flow.

Appendix A. List of Integrals Used and Their Solutions

Integral I_1

The integral I_1 is given by

$$I_1(a,b,c,d) = \int_a^b \frac{b-z}{b-a} \ln \sqrt{(z-c)^2+d^2} dz \tag{A.1}$$

where $a \neq b$ and $d \geq 0$.

Muleshkov solves $I_1(a,b,c,d)$ for all possible cases of a, b, c, and d in his doctoral dissertation, "Analytical and Numerical Determination of Steady Seepage Toward Vertical Cuts," on pages 94-95 (1988). The evaluation and notation of I_1 are directly from his dissertation.

For the most general case of I_1 when $d > 0$, Eq. A.1 becomes

$$I_1(a,b,c,d) = \frac{(a-c)(a-2b+c)+d^2}{2(b-a)} \ln \sqrt{(a-c)^2+d^2} + \frac{1}{4}(a-3b+2c) +$$

$$\frac{(b-c)^2-d^2}{2(b-a)} \ln \sqrt{(b-c)^2+d^2} + \frac{d(b-c)}{b-a}(\arctan \frac{b-c}{d} - \arctan \frac{a-c}{d}) \tag{A.2}$$

When $a \neq b \neq c$ and finding the limit as $d \to 0$, Eq. A.2 becomes

$$I_1(a,b,c,0) = \frac{(a-c)(a-2b+c)}{2(b-a)} \ln|a-c| + \frac{(b-c)^2}{2(b-a)} \ln|b-c| + \frac{1}{4}(a-3b+2c) \tag{A.3}$$

When $c \to a$ and $d = 0$, Eq. A.3 becomes

$$I_1(a,b,a,0) = \frac{1}{2}(b-c) \ln|b-a| + \frac{3}{4}(a-b) \tag{A.4}$$

From Eq. A.4, when $c \to b$ and $d = 0$, on gets

$$I_1(a,b,b,0) = \frac{1}{2}(b-a)\ln|b-a| + \frac{1}{4}(a-b) \tag{A.5}$$

Integral I_2

The integral I_2 is given by

$$I_2(a,b,c,d) = \int_a^b \frac{b-z}{b-a} \cdot \frac{d}{(z-c)^2+d^2} dz \tag{A.6}$$

where $a \neq b$.Muleshkov solves $I_2(a,b,c,d)$ for all possible cases of a, b, c, and d in his doctoral dissertation, "Analytical and Numerical Determination of Steady Seepage Toward Vertical Cuts," on pages 95-96 (1988). The evaluation and notation of I_2 are directly from his dissertation.

For the most general case $d \neq 0$, Eq. A.6 becomes

$$I_2(a,b,c,d) = \frac{b-c}{b-a}(\arctan\frac{b-c}{d} - \arctan\frac{a-c}{d}) -$$

$$\frac{d}{b-a}\ln\sqrt{(b-c)^2+d^2} + \frac{d}{b-a}\ln\sqrt{(a-c)^2+d^2} \tag{A.7}$$

When $d = 0$, Eq. A.7 becomes

$$I_2(a,b,c,0) = 0 \tag{A.8}$$

Integral I_3

The integral I_3 is given by

$$I_3(a,b,c,d) = d\int_a^b \frac{dz}{(z-c)^2+d^2} \tag{A.9}$$

where $a \neq b$.Muleshkov solves $I_3(a,b,c,d)$ for all possible cases of a, b, c, and d in his doctoral dissertation, "Analytical and Numerical Determination of Steady Seepage Toward Vertical Cuts," on page 96 (1988). The evaluation and notation of I_3 are directly from his dissertation.

The most general case, when $d \neq 0$ Eq. A.9 becomes,

$$I_3(a,b,c,d) = \arctan\frac{b-c}{d} - \arctan\frac{a-c}{d} \tag{A.10}$$

When $d = 0$, from Eq. A.10 one gets,

$$I_3(a,b,c,0) = 0 \tag{A.11}$$

Integral I_4

The integral I_4 is given by

$$I_4(a,b,c) = c\int_0^c z\ln[(z^3-a)^2+b^2]dz \tag{A.12}$$

where $a \neq b$ and $b \geq 0$. Muleshkov solves $I_4(a,b,c)$ for all possible cases of a, b, c, and d in his doctoral dissertation, "Analytical and Numerical Determination of Steady Seepage Toward Vertical Cuts," on pages 96-101 (1988). The evaluation and notation of I_4 are directly from his dissertation.

For the most general case, $b > 0$ is given by

$$I_4(a,b,c) = \frac{c^3}{2}\ln[(c^3-a)^2+b^2] - \frac{3}{2}c^3 - c\lambda^2\sum_{k=-1}^{1}(2\mu_k^2-1)\ln\sqrt{1-2\mu_k\frac{c}{\lambda}+\frac{c^2}{\lambda^2}}$$

$$+2c\lambda^2\sum_{k=-1}^{1}\mu_k\bar{\mu_k}(\arctan\frac{c-\lambda\mu_k}{\lambda\bar{\mu_k}} + \arctan\frac{\mu_k}{\bar{\mu_k}}) \tag{A.13}$$

Where

$\lambda = \sqrt[6]{a^2+b^2}$

$\theta = \frac{1}{3}\arccos\frac{a}{\lambda^3}$

$\mu_k = \cos(\theta + \frac{2k\pi}{3})$, $k = -1, 0, 1$

$\bar{\mu_k} = \sin(\theta + \frac{2k\pi}{3})$, $k = -1, 0, 1$

When $b \to 0$, Eq. A.13 becomes

$$I_4(a,0,c) = c^3 \ln|c^3 - a| - 1.5c^3 - c\sqrt[3]{a^2}[\frac{1}{2}\ln\frac{(c-\sqrt[3]{a})^3}{c^3-a} + \sqrt{3}\arctan(\frac{1}{\sqrt{3}} + \frac{2c}{\sqrt{3}\sqrt[3]{a}} - \frac{\pi}{2\sqrt{3}}] \tag{A.14}$$

Lastly, from Eq. A.14, when $c \to \sqrt[3]{a}$, one gets,

$$I_4(a,0,\sqrt[3]{a}) = a\ln|a| + \frac{3}{2}a\ln 3 - \frac{\pi a}{2\sqrt{3}} - \frac{3}{2}a \tag{A.15}$$

Integral I_5

The integral I_5 is given by

$$I_5(a,b,c) = \frac{3b}{c^4}\int_0^c \frac{z^6}{(z^3-a)^2+b^2}dz \tag{A.16}$$

where $c \neq 0$. Muleshkov solves $I_5(a,b,c)$ for all possible cases of a, b, c, and d in his doctoral dissertation, "Analytical and Numerical Determination of Steady Seepage Toward Vertical Cuts," on pages 102-107 (1988). The evaluation and notation of I_5 are directly from his dissertation.

In the most general case, $b > 0$ is given by

$$I_5(a,b,c) = \frac{3b}{c^3} + \frac{\lambda^4}{c^4}\sum_{k=-1}^{1}(\bar{v_k}\ln\sqrt{1 - 2\mu_k\frac{c}{\lambda} + \frac{c^2}{\lambda^2}} + v_k(\arctan\frac{\frac{c}{\lambda} - \mu_k}{\bar{\mu_k}} + \arctan\frac{\mu_k}{\bar{\mu_k}}) \tag{A.17}$$

Where

$\lambda = \sqrt[6]{a^2+b^2}$

$\theta = \frac{1}{3}\arccos\frac{a}{\lambda^3}$

$\mu_k = \cos(\theta + \frac{2k\pi}{3}),\ k = -1, 0, 1$

$\bar{\mu_k} = \sin(\theta + \frac{2k\pi}{3}),\ k = -1, 0, 1$

$v_k = \cos(4\theta + \frac{2k\pi}{3}), k = -1, 0, 1$

$\bar{v_k} = \sin(\theta + \frac{2k\pi}{3}), k = -1, 0, 1$

When $b \to 0$, Eq. A.17 becomes

$$I_5(a,0,c) \to \frac{b}{c^4}(3c + \frac{ac}{a-c^3} + \frac{2\sqrt[3]{a}}{a-c^3}\ln\frac{(c-\sqrt[3]{a})^3}{c^3-a} - \frac{4\sqrt[3]{a}}{\sqrt{3}}(\arctan(\frac{2c}{\sqrt{3}\sqrt[3]{a}} + \frac{1}{\sqrt{3}}) - \frac{\pi}{6}) \tag{A.18}$$

and as $a \to c^3$ Eq. A.18 becomes

$$I_5(c^3,0,c) = 0 \tag{A.19}$$

Integral I_6

The integral I_6 is given by

$$I_6(a,b,c) = \frac{3}{2c}\int_0^c z^3 \ln[(z^3-a)^2 + b^2]dz \tag{A.20}$$

where $a \neq b$ and $b \geq 0$. Muleshkov solves $I_6(a,b,c)$ for all possible cases of a, b, c, and d in his doctoral dissertation, "Analytical and Numerical Determination of Steady Seepage Toward Vertical Cuts," on pages 102-107 (1988). The evaluation and notation of I_6 are directly from his dissertation.

For the most general case, $b > 0$ is given by

$$I_6(a,b,c) = \frac{3c^3}{8}\ln[(c^3-a)^2+b^2] - \frac{9}{16}c^3 - \frac{9}{4}a + \frac{3}{4c}\lambda^4 \sum_{k=-1}^{1}(-v_k \ln\sqrt{1 - 2\mu_k\frac{c}{\lambda} + \frac{c^2}{\lambda^2}}$$

$$+\bar{v_k}(\arctan\frac{\frac{c}{\lambda} - \mu_k}{\bar{\mu_k}} + \arctan\frac{\mu_k}{\bar{\mu_k}})) \tag{A.21}$$

Where

$\lambda = \sqrt[6]{a^2+b^2}$

$\theta = \frac{1}{3}\arccos\frac{a}{\lambda^3}$

$\mu_k = \cos(\theta + \frac{2k\pi}{3})$, $k = -1, 0, 1$

$\bar{\mu_k} = \sin(\theta + \frac{2k\pi}{3})$, $k = -1, 0, 1$

$v_k = \cos(4\theta + \frac{2k\pi}{3}), k = -1, 0, 1$

$\bar{v_k} = \sin(\theta + \frac{2k\pi}{3}), k = -1, 0, 1$

When $b \to 0$ and $c \neq \sqrt[3]{a}$, Eq. A.21 becomes

$$I_6(a, 0, c) = \frac{3}{4}c^3 \ln|c^3 - a| - \frac{9}{16}c^3 - \frac{9}{4}a - \frac{3}{4c}\sqrt[3]{a^4} \ln|\frac{c}{\sqrt[3]{a}} - 1| +$$

$$\frac{3}{8c}\sqrt[3]{a^4} \ln|1 + \frac{c}{\sqrt[3]{a}} + \frac{c^2}{\sqrt[3]{a^2}}| + \frac{3\sqrt{3}}{4c}\sqrt[3]{a^4} \arctan(\frac{1}{\sqrt{3}} + \frac{2c}{\sqrt{3}\sqrt[3]{a}}) - \frac{\pi\sqrt{3}}{8}\sqrt[3]{a^4} \quad \text{(A.22)}$$

Lastly, when $b \to 0$ and $c \to \sqrt[3]{a}$, Eq. A.22 becomes

$$I_6(a, 0, \sqrt[3]{a}) = \frac{9}{8}c^3(\ln c^2 + \ln 3 - 2.5 + \frac{\pi}{3\sqrt{3}}) \quad \text{(A.23)}$$

Integral I_7

The integral I_7 is given by

$$I_7(a, b, c, d) = -\int_a^b \ln\sqrt{(z - c)^2 + d^2}dz$$

where $a \neq b$ and $d \geq 0$. Muleshkov solves $I_7(a, b, c, d)$ for all possible cases of a, b, c, and d in his doctoral dissertation, "Analytical and Numerical Determination of Steady Seepage Toward Vertical Cuts," on pages 107-108 (1988). The evaluation and notation of I_7 are directly from his dissertation.

The most general case is solved for $d \neq 0$ and is given by

$$I_7(a, b, c, d) = (c - b) \ln\sqrt{(b - c)^2 + d^2} - (c - a) \ln\sqrt{(a - c)^2 + d^2} +$$

$$b - a - d \arctan\frac{b - c}{d} + d \arctan\frac{a - c}{d} \quad \text{(A.24)}$$

When $d \to 0$ and $a \neq b \neq c$, Eq. A.24 turns into

$$I_7(a,b,c,0) = (c-b)\ln|c-b| - (c-a)\ln|c-a| + b - a \tag{A.25}$$

Next as $d \to 0$ and $c \to a$ and $a \neq b$, Eq. A.25 turns into

$$I_7(a,b,a,0) = (a-b)\ln|a-b| + b - a \tag{A.26}$$

In addition, when $d \to 0$ and $c \to b$ and $a \neq b$, A.25 turns into

$$I_7(a,b,b,0) = (a-b)\ln|a-b| + b - a \tag{A.27}$$

Lastly, as $d \to 0$, $c \to a$, and $a = b$, Eq. A.27 becomes

$$I_7(a,a,a,0) = 0 \tag{A.28}$$

Integral I_8

The integral I_8 is given by

$$I_8(a,b,c) = \frac{2b}{c}\int_0^c \frac{z^2}{(z^2-a)^2+b^2}dz \tag{A.29}$$

where $c \neq 0$. I_8 is first solved by partial fractions for the most general case of a, b, c where $c \neq \sqrt{a}$ and $b \neq 0$.

Expanding the denominator of the integrand of Eq. A.29 and then factoring one gets,

$$(z^2-a)^2+b^2 = z^4 - 2az^2 + a^2 + b^2 = z^4 + a^2 + b^2 + 2z^2\sqrt{a^2+b^2} - z^2(2a + 2a\sqrt{a^2+b^2})$$

$$= (z^2 + \sqrt{a^2+b^2} - z\sqrt{2a+2\sqrt{a^2+b^2}})(z^2 + \sqrt{a^2+b^2} + z\sqrt{2a+2\sqrt{a^2+b^2}}) \tag{A.30}$$

Using the notations

$$\alpha = \sqrt{2a + 2\sqrt{a^2 + b^2}} \tag{A.31}$$

$$\beta = \sqrt{a^2 + b^2} \tag{A.32}$$

Eq. A.30 becomes,

$$(z^2-a)^2+b^2 = (z^2+\sqrt{a^2+b^2}-z\sqrt{2a+2\sqrt{a^2+b^2}})(z^2+\sqrt{a^2+b^2}+z\sqrt{2a+2\sqrt{a^2+b^2}}) =$$

$$(z^2 + \alpha z + \beta)(z^2 - \alpha z + \beta) \tag{A.33}$$

Using Eq. A.33, the integrand of Eq. A.29 becomes

$$\frac{z^2}{(z^2 + \alpha z + \beta)(z^2 - \alpha z + \beta)} = \frac{Az + B}{(z^2 + \alpha z + \beta)} + \frac{Cz + D}{(z^2 - \alpha z + \beta)} \tag{A.34}$$

Then one gets,

$$z^2 = (Az + B)(z^2 - \alpha z + \beta) + (Cz + D)(z^2 - \alpha z + \beta) \tag{A.35}$$

where A, B, C, and D are real valued constants. By comparing the coefficients of corresponding powers on the left hand side to the right hand side in Eq. A.35, one gets $A = \frac{-1}{2\alpha}, B = 0, C = \frac{1}{2\alpha}$, and $D = 0$.

Therefore, Eq. A.34 becomes

$$\frac{z^2}{(z^2 + \alpha z + \beta)(z^2 - \alpha z + \beta)} = \frac{-1}{2\alpha} \cdot \frac{z}{z^2 + \alpha z + \beta} + \frac{1}{2\alpha} \cdot \frac{z}{z^2 - \alpha z + \beta} \tag{A.36}$$

Thus, to find the solution of Eq. A.29 in the most general case,

$$I_8(a,b,c) = \frac{2b}{c}\int_0^c \frac{z^2}{(z^2-a)^2+b^2}dz = \frac{2b}{c}(\frac{-1}{2\alpha}\int_0^c \frac{z}{z^2+\alpha z+\beta}dz + \frac{1}{2\alpha}\int_0^c \frac{z}{z^2-\alpha z+\beta}dz)$$

$$\implies I_8(a,b,c) = \frac{2b}{c}(\frac{1}{4\alpha}(\ln|z^2-\alpha z+\beta| - \ln|z^2+\alpha z+\beta|)$$

$$+\frac{1}{2\sqrt{4\beta-\alpha^2}}(\arctan\frac{2z+\alpha}{\sqrt{4\beta-\alpha^2}} + \arctan\frac{2z-\alpha}{\sqrt{4\beta-\alpha^2}}))\Big|_0^c \tag{A.37}$$

Evaluating Eq. A.37, one gets

$$I_8(a,b,c) = \frac{2b}{c}(\frac{1}{4\alpha}(\ln|c^2-\alpha c+\beta| - \ln|c^2+\alpha c+\beta|)+$$

$$\frac{1}{2\sqrt{4\beta-\alpha^2}}(\arctan\frac{2c+\alpha}{\sqrt{4\beta-\alpha^2}} + \arctan\frac{2c-\alpha}{\sqrt{4\beta-\alpha^2}})) \tag{A.38}$$

where α and β are given in Eq. A.31 and Eq. A.32.

Eq. A.29 must be solved for a special where the integral is singular, namely when $b \to 0$ and $c = \sqrt{a}$. The asymptotic approximation of Eq. A.31 and Eq. A.32 are given to find the partial fraction decomposition of the integrand in Eq. A.29.

From Eq. A.32,

$$\sqrt{a^2+b^2} \sim a(1+\frac{b^2}{a^2})^{1/2} \sim a(1+\binom{1}{1/2}\frac{b^2}{a^2}) = a + \frac{ab^2}{2a^2} = a + \frac{b^2}{2a} \tag{A.39}$$

and from Eq. A.31 using Eq. A.39,

$$2a+2\sqrt{a^2+b^2} \sim 4a+\frac{b^2}{a} \implies \sqrt{2a+2\sqrt{a^2+b^2}} \sim \sqrt{4a+\frac{b^2}{a}} = 2\sqrt{a}(1+\frac{b^2}{4a^2})^{\frac{1}{2}} \sim 2\sqrt{a}(1+\frac{b^2}{8a^2}) \tag{A.40}$$

Then the denominator of the integrand in Eq. A.29 becomes

$$(z^2-a)^2+b^2 = (z^2+\sqrt{a^2+b^2}-z\sqrt{2a+2\sqrt{a^2+b^2}})(z^2+\sqrt{a^2+b^2}+z\sqrt{2a+2\sqrt{a^2+b^2}}) \sim$$

$$((z+\sqrt{a}+\frac{b^2}{8a\sqrt{a}})^2+\frac{b^2}{4a})((z-(\sqrt{a}+\frac{b^2}{8a\sqrt{a}}))^2+\frac{b^2}{4a}) \tag{A.41}$$

Next, one can use Eq. A.41 to find the partial fraction decomposition of the integrand in Eq. A.29,

$$\frac{z^2}{((z+\sqrt{a}+\frac{b^2}{8a\sqrt{a}})^2+\frac{b^2}{4a})((z-(\sqrt{a}+\frac{b^2}{8a\sqrt{a}}))^2+\frac{b^2}{4a})} =$$

$$\frac{Ez+F}{((z+\sqrt{a}+\frac{b^2}{8a\sqrt{a}})^2+\frac{b^2}{4a})}+\frac{Gz+H}{(z-(\sqrt{a}+\frac{b^2}{8a\sqrt{a}}))^2+\frac{b^2}{4a})} \tag{A.42}$$

where E, F, G and H are real constants.

From Eq. A.42

$$z^2 = (Ez+F)((z-(\sqrt{a}+\frac{b^2}{8a\sqrt{a}}))^2+\frac{b^2}{4a}))+(Gz+H)((z+\sqrt{a}+\frac{b^2}{8a\sqrt{a}})^2+\frac{b^2}{4a}) \tag{A.43}$$

by comparing the coefficients of corresponding powers on the left hand side to the right hand side of Eq. A.43, one gets $E=\frac{-1}{4(\sqrt{a}+\frac{b^2}{8\sqrt{a}})}$, $F=0$, $G=\frac{1}{4(\sqrt{a}+\frac{b^2}{8\sqrt{a}})}$, and $H=0$.

Hence, one gets

$$I_8(a,b,c) = \frac{2b}{c}\int_0^c \frac{z^2}{(z^2-a)^2+b^2}dz \sim \frac{2b}{c}(\frac{-1}{4(\sqrt{a}+\frac{b^2}{8\sqrt{a}})}\int_0^c \frac{z}{(z+\sqrt{a}+\frac{b^2}{8a\sqrt{a}})^2+\frac{b^2}{4a})}dz+$$

$$\frac{1}{4(\sqrt{a}+\frac{b^2}{8\sqrt{a}})}\int_0^c \frac{z}{(z-(\sqrt{a}+\frac{b^2}{8a\sqrt{a}}))^2+\frac{b^2}{4a})})dz$$

$$\implies I_8(a,b,c) \sim \frac{b}{4c(\sqrt{a}+\frac{b^2}{8a\sqrt{a}})}(\ln|(z+\sqrt{a}+\frac{b^2}{8a\sqrt{a}})^2+\frac{b^2}{4a}|-\ln|(z-(\sqrt{a}+\frac{b^2}{8a\sqrt{a}}))^2+\frac{b^2}{4a})|)+$$

$$\frac{\sqrt{a}}{2c}(\arctan\frac{2\sqrt{a}(z+\sqrt{a}+\frac{b^2}{8a\sqrt{a}})}{b}+\arctan\frac{2\sqrt{a}(z-(\sqrt{a}+\frac{b^2}{8a\sqrt{a}}))}{b})\Big|_0^c \tag{A.44}$$

Then, evaluating Eq. A.44

$$I_8(a,b,c) \sim \frac{b}{4c(\sqrt{a}+\frac{b^2}{8a\sqrt{a}})}(\ln|(c+\sqrt{a}+\frac{b^2}{8a\sqrt{a}})^2+\frac{b^2}{4a}|-\ln|(c-(\sqrt{a}+\frac{b^2}{8a\sqrt{a}}))^2+\frac{b^2}{4a})|)$$

$$\frac{\sqrt{a}}{c}(\arctan\frac{2\sqrt{a}(c+\sqrt{a}+\frac{b^2}{8a\sqrt{a}})}{b}+\arctan\frac{2\sqrt{a}(c-(\sqrt{a}+\frac{b^2}{8a\sqrt{a}}))}{b}) \tag{A.45}$$

From Eq. A.45, when $b \to 0$ and $c = \sqrt{a}$, I_8 becomes

$$I_8(a,b,\sqrt{a}) \sim \frac{\pi}{2}$$

Integral I_9

The integral I_9 is given by

$$I_9(a,b,c) = c\int_0^c \ln((z^2-a)^2+b^2)dz \tag{A.46}$$

where $b \geq 0$ and $c \neq 0$ and will be solved for all possible cases of a, b, and c. First, when $a \geq c^2$ and $0 \leq a$, for $b > 0$.

Using the notations from Eq. A.31 and Eq. A.32 one needs

$$\frac{1}{(z^2+\alpha z+\beta)(z^2-\alpha z+\beta)} = \frac{1}{2\beta\alpha}\cdot\frac{z+\alpha}{(z^2+\alpha z+\beta)} - \frac{1}{2\beta\alpha}\cdot\frac{z-\alpha}{(z^2-\alpha z+\beta)} \tag{A.47}$$

in order to find the solution of Eq. A.46

Integrating by parts, one gets

$$I_9(a,b,c) = c(z\ln((z^2-a)^2+b^2)\Big|_0^c - 4\int_0^c \frac{z^4-az^2}{(z^2-a)^2+b^2}dz) \Longrightarrow$$

$$I_9(a,b,c) = c(z\ln((z^2-a)^2+b^2)\Big|_0^c - 4\int_0^c dz + 4\int_0^c \frac{a^2+b^2}{(z^2-a)^2+b^2}dz - 4a\int_0^c \frac{z^2}{(z^2-a)^2+b^2}dz \tag{A.48}$$

From Eq. A.47,

$$I_9(a,b,c) = c(z\ln((z^2-a)^2+b^2)\Big|_0^c - 4\int_0^c dz + \frac{4c(a^2+b^2)}{2\beta\alpha}\int_0^c \frac{z+\alpha}{(z^2+\alpha z+\beta)}dz -$$

$$\frac{4c(a^2+b^2)}{2\beta\alpha}\int_0^c \frac{z-\alpha}{(z^2-\alpha z+\beta)}dz - 4a\int_0^c \frac{z^2}{(z^2-a)^2+b^2}dz) \tag{A.49}$$

Evaluating the integrals in Eq. A.49, I_9 becomes,

$$I_9(a,b,c) = c^2\ln|(c^2-a)^2+b^2| - 4c - 4ac(\frac{1}{4\alpha}(\ln|c^2-\alpha c+\beta| - \ln|c^2+\alpha c+\beta|) +$$

$$\frac{1}{2\sqrt{4\beta-\alpha^2}}(\arctan\frac{2c+\alpha}{\sqrt{4\beta-\alpha^2}} + \arctan\frac{2c-\alpha}{\sqrt{4\beta-\alpha^2}})) +$$

$$c\frac{a^2+b^2}{\alpha\beta}\ln\frac{|c^2+\alpha c+\beta|}{|c^2-\alpha c+\beta|} + \frac{2c(a^2+b^2)}{\beta\sqrt{4\beta-\alpha^2}}(\arctan\frac{2c+\alpha}{\sqrt{4\beta-\alpha^2}} - \arctan\frac{2c-\alpha}{\sqrt{4\beta-\alpha^2}}) \tag{A.50}$$

where $\int_0^c \frac{z^2}{(z^2-a)^2+b^2}dz$ has been evaluated in Eq. A.38.

For $b = 0$ and $c \neq \sqrt{a}$, I_9 can be evaluated directly from Eq. A.46,

$$I_9(a,b,c) = I_9(a,0,c) = 2c\int_0^c \ln(z^2-a)dz \tag{A.51}$$

Integrating by parts one gets,

$$\frac{1}{2c}I_9(a,0,c) = z\ln(z^2-a)\Big|_0^c - 2\int_0^c \frac{z^2}{z^2-a}dz$$

$$\Longrightarrow \frac{1}{2c}I_9(a,0,b) = z\ln(z^2-a)\Big|_0^c - 2\int_0^c dz - 2\int_0^c \frac{a}{z^2-a}dz = z\ln(z^2-a) - 2z - \sqrt{a}\ln|\frac{z-\sqrt{a}}{z+\sqrt{a}}|\Big|_0^c$$

Hence, the formula can be obtained,

$$I_9(a,0,c) = 2c^2\ln(c^2-a) - 4c^2 - 2c\sqrt{a}\ln|\frac{c-\sqrt{a}}{c+\sqrt{a}}| \tag{A.52}$$

When $b = 0$ as $c \to \sqrt{a}$ from Eq. A.52, one gets,

$$I_9(a,b,c) \to 2a\ln|4a| - 4a \tag{A.53}$$

Integral I_{10}

The integral I_{10} is given by,

$$I_{10}(a,b,c) = \frac{b}{c}\int_0^c \frac{z^2}{(z-a)^2+b^2}dz \tag{A.54}$$

where $c \neq 0$ and I_{10} will be solved for all possible cases of a, b, and c. First, it will be solved in the most general case for $b \neq 0$ and $c \neq a$.

For $\frac{z^2}{(z-a)^2+b^2}$,the power of the numerator is equal to the power of the denominator, one should first divide

$\frac{z^2}{(z-a)^2+b^2} = 1 + \frac{2az}{(z-a)^2+b^2} - (a^2+b^2)\frac{1}{(z-a)^2+b^2} = 1 + 2a\frac{(z-a)}{(z-a)^2+^2} + (a^2-b^2)\frac{1}{(z-a)^2+b^2}$

Then, Eq. A.54 becomes,

$$I_{10}(a,b,c) = \frac{b}{c}\int_0^c dz + \frac{ab}{c}\int_0^c \frac{2(z-a)}{(z-a)^2+b^2}dz + \frac{(a^2-b^2)b}{c}\int_0^c \frac{dz}{(z-a)^2+b^2} \tag{A.55}$$

and then integrating, one gets,

$$I_{10}(a,b,c) = \frac{b}{c}z + \frac{ab}{c}\ln|(z-a)^2+b^2| + \frac{(a^2-b^2)}{c}\arctan\frac{z-a}{b}\Bigg|_0^c \tag{A.56}$$

and lastly, evaluating the limits, one gets,

$$I_{10}(a,b,c) = b+\frac{ab}{c}\ln|(c-a)^2+b^2|+\frac{(a^2-b^2)}{c}\arctan\frac{c-a}{b}-\frac{ab}{c}\ln|a^2+b^2|+\frac{(a^2-b^2)}{c}\arctan\frac{a}{b} \tag{A.57}$$

As $b \to 0$ and $c = a$, from Eq. A.57 one gets,

$$I_{10}(a,b,a) \to \frac{a\pi}{2} \tag{A.58}$$

Integral I_{11}

The integral I_{11} is given by

$$I_{11}(a,b,c,d) = a\int_a^b \frac{1}{z}\ln\sqrt{(z-c)^2+d^2}dz \tag{A.59}$$

which is solved numerically using Mathematica (Wolfram Research, Inc., 2018).

Integral I_{12}

The integral I_{12} is given by

$$I_{12}(a,b,c) = \frac{3b}{c^2}\int_0^c \frac{z^4}{(z^3-a)^2+b^2}dz \tag{A.60}$$

where $c \neq 0$. The solution of Eq. A.60 is not trivial. Computer software (Wolfram Research, Inc., 2018) can solve the problem exactly when $c \neq \sqrt[3]{a}$ and $b \neq 0$. However, Eq. A.60 is singular when $b \to 0$ and $c = \sqrt[3]{a}$. Hence, we will only find the solution of I_{12} for this case.

From the substitutions, $t = \frac{z}{\sqrt[3]{b}}$ and $\alpha = \sqrt[3]{\frac{a}{b}}$, Eq. A.60 becomes

$$\frac{c^2}{3} I_{12}(a,b,c,d) = \frac{\sqrt[3]{a^2}}{\alpha^2} \int_0^{\frac{c\alpha}{\sqrt[3]{a}}} \frac{t^4}{(t^3-\alpha^3)^2+1} dt \tag{A.61}$$

Using $\beta = \frac{1}{\alpha^3}$, Eq. A.61 becomes

$$\frac{c^2}{3} I_{12}(a,\beta,c) = \beta^{\frac{2}{3}} \sqrt[3]{a^2} \int_0^{\frac{c}{\sqrt[3]{a}\sqrt[3]{\beta}}} \beta^2 t^4 \frac{1}{\beta^2(t^6+1) - 2\beta t^3 + 1} dt \tag{A.62}$$

Now, one is interested in evaluating Eq. A.62 as $\beta \to 0^+$. To do that, one can find the series expansion of

$$E = \frac{1}{1 - 2t^3 + (t^6+1)\beta^2} = 1 + A\beta + B\beta^2 + ...$$

$$\implies 1 = (1 + A\beta + B\beta^2 + ...)(1 - 2t^3 + (t^6+1)\beta^2) \tag{A.63}$$

From Eq. A.63

$$1 = 1 \tag{A.64}$$

$$0 = A - 2t^3 \implies A = 2t^3 \tag{A.65}$$

$$0 = B - 2At^3 + t^6 + 1 = B - 2(2t^3)t^3 + t^6 + 1 \implies B = 3t^6 - 1 \tag{A.66}$$

Then from Eqs. A.64-A.66, Eq. A.63 becomes

$$E = 1 + 2t^3\beta + (3t^6 - 1)\beta^2 + ... \tag{A.67}$$

From Eq. A.67, Eq. A.62 becomes

$$\frac{c^2}{3} I_{12}(a,\beta,c) = \beta^{\frac{8}{3}a^{2/3}} \int_0^{\frac{c}{\sqrt[3]{a}\sqrt[3]{\beta}}} t^4(1 + 2t^3\beta + (3t^6-1)\beta^2 + ...) dt$$

$$= \beta^{\frac{8}{3}} a^{\frac{2}{3}} [\frac{t^5}{5} + \frac{t^8}{4}\beta + \frac{3t^{11}}{11}\beta^2 - \frac{t^5}{5}\beta^2 + ...]\Big|_0^{\frac{c}{\sqrt[3]{a}\sqrt[3]{\beta}}}$$

$$= \beta^{\frac{8}{3}} a^{\frac{2}{3}} [\frac{c^5}{5a^{\frac{5}{3}}\beta^{\frac{5}{3}}} + \frac{c^8}{4a^{\frac{8}{3}}\beta^{\frac{8}{3}}}\beta + \frac{3c^{11}}{11a^{\frac{11}{3}}\beta^{\frac{11}{3}}}\beta^2 - \frac{c^5}{5a^{\frac{5}{3}}\beta^{\frac{5}{3}}}\beta^2 + ...]$$

$$= \frac{c^5}{5a}\beta + \frac{c^8}{4a^2}\beta + \frac{3c^{11}}{11a^3}\beta - \frac{c^5}{5a}\beta^3 + ... \tag{A.68}$$

As $\beta \to 0^+$, Eq. A.68 becomes

$$\frac{c^2}{3} I_{12}(a, \beta, c) \to 0$$

Hence,

$$I_{12}(a, b, c) \to 0 \tag{A.69}$$

as $b \to 0$.

Therefore, for I_{12} when $b \to 0$ and $c = \sqrt[3]{a}$,

$$I_{12}(a, 0, \sqrt[3]{a}) \to 0 \tag{A.70}$$

Integral I_{13}

The integral I_{13} is given by

$$I_{13}(a, b, c) = \frac{1}{2c} \int_0^c z \ln((z-a)^2 + b^2) dz \tag{A.71}$$

where $b \geq 0$ and $c \neq 0$ and will be solved for all cases of a, b, and c. First, for the case of $b > 0$ the integral,

$$\widetilde{I}_{13}(a, b, c) = \int_0^c (z-a) \ln((z-a)^2 + b^2) dz \tag{A.72}$$

will be solved. It is clear that Eq. A.72 becomes

$$\widetilde{I}_{13}(a,b,c) = \frac{1}{2}\int_{a^2+b^2}^{(c-a)^2+b^2} \ln|u|du \tag{A.73}$$

Then, integrating by parts one gets,

$$\widetilde{I}_{13}(a,b,c) = \frac{1}{2}u\ln u\Big|_{a^2+b^2}^{(c-a)^2+b^2} - \int_{a^2+b^2}^{(c-a)^2+b^2} 1du = \frac{1}{2}u\ln u - \frac{1}{2}u\Big|_{a^2+b^2}^{(c-a)^2+b^2} \Longrightarrow$$

$$\widetilde{I}_{13}(a,b,c) = \frac{1}{2}(((c-a)^2+b^2)\ln((c-a)^2+b^2) - (a^2+b^2)\ln(a^2+b^2) - (c-a)^2 - b^2 + a^2 + b^2) \tag{A.74}$$

Now, back to Eq. A.71, adding a to z and subtracting a from z, one gets,

$$I_{13}(a,b,c) = \frac{1}{2c}\int_0^c (z-a)\ln((z-a)^2+b^2)dz + \frac{a}{2c}\int_0^c \ln((z-a)^2+b^2)dz =$$

$$= \frac{1}{2c}\widetilde{I}_{13}(a,b,c) + \frac{a}{2c}\int_0^c \ln((z-a)^2+b^2)dz = \frac{1}{2c}\widetilde{I}_{13}(a,b,c) + \frac{a}{c}\int_0^c \ln\sqrt{(z-a)^2+b^2}dz \Longrightarrow$$

$$I_{13}(a,b,c) = \frac{1}{4c}(((c-a)^2+b^2)\ln((c-a)^2+b^2) - (a^2+b^2)\ln(a^2+b^2) -$$

$$(c-a)^2 - b^2 + a^2 + b^2) - \frac{a}{c}I_7(0,c,a,b) \tag{A.75}$$

where I_7 has been solved for all possible cases in Eqs. A.24-A.28.

For the case when $b = 0$ and $c \neq a$, Eq. A.71 becomes,

$$I_{13}(a,0,c) = \frac{1}{2c}\int_0^c z\ln(z-a)^2 dz \tag{A.76}$$

Adding a to z and subtracting a from z, one gets,

$$I_{13}(a,0,c) = \frac{1}{2c}\int_0^c (z-a)\ln(z-a)^2 dz + \frac{a}{2c}\int_0^c \ln(z-a)^2 dz =$$

$$\frac{1}{4c}\int_{a^2}^{(c-a)^2} \ln|u| dz + \frac{a}{c}\int_{-a}^{c-a} \ln|u| dz \tag{A.77}$$

Integrating by parts, one gets

$$I_{13}(a,0,c) = \frac{1}{4c}(u\ln|u| - u)\Big|_{a^2}^{(c-a)^2} + \frac{a}{c}(u\ln|u| - u)\Big|_{-a}^{(c-a)}$$

Evaluating the limits, one gets,

$$I_{13}(a,0,c) = \frac{1}{4c}((c-a)^2\ln(c-a)^2 - a^2\ln a^2 - (c-a)^2 + a^2) +$$

$$\frac{a}{c}((c-a)\ln|c-a| - (c-a) + a\ln|a| - a) \tag{A.78}$$

The case when $b = 0$ and $c \to a$, can be found by evaluating the limit $c \to a$ in Eq. A.78,

$$I_{13}(a,0,c) \to \frac{a^2}{2c}\ln|a| - \frac{3a^2}{4c} \tag{A.79}$$

References

Abramowitz, M., & Stegun, I. A. (2013). Handbook of mathematical functions: With formulas, graphs, and mathematical tables. New York, NY: Dover Publ.

Bruch, E. K. (1991). The boundary element method for groundwater flow. Berlin u.a: Springer.

Carrier, G. F., Krook, M., & Pearson, C. E. (2005). Functions of a complex variable: Theory and practice. Philadelphia, Pa: Society for Industrial and Applied Mathematics.

Cedergren, H. R. (1967). Seepage, drainage, and flow nets. New York: Wiley.

Harr, M. E. (1990). Groundwater and seepage. New York: Dover.

Igarashi, H., & Honma, T. (January 01, 1996). A boundary element method for potential fields with corner singularities. Applied Mathematical Modelling, 20, 11, 847-852.

Kythe, P. K. (1995). An introduction to boundary element methods. Boca Raton: CRC Press.

Lecture 6. (n.d.). Retrieved June 20, 2018, from https://hydro.geo.ua.edu/GEO406_506/Lecture6.pdf

Lefeber, D. (1989). Solving problems with singularities using boundary elements. Southampton, UK: Computational Mechanics Publications.

Liggett, J. A., & Liu, P. L.-F. (1983). The boundary integral equation method for porous media flow. London: Allen & Unwin.

Mathews, J. H., & Howell, R. W. (2012). Complex analysis for mathematics and engineering. Boston: Jones and Bartlett.

Muleshkov, A. (1988). Analytical and numerical determination of steady seepage towards vertical cuts.

Muleshkov, A. (2016). Lectures on Conformal Mapping. Personal Collection of A. Muleshkov, University of Nevada, Las Vegas, Las Vegas, NV.

Polubarinova-Kochina, P. I. A. (1962). Theory of water movement. Princeton, N.J: Princeton University Press.

Wolfram Research, Inc. (2018). Mathematica. Champaign, IL: Wolfram Research, Inc.

Curriculum Vitae

Graduate College

University of Nevada, Las Vegas

Megan Ann Romero

Degrees:

Bachelor of Science in Mathematics, 2013

University of Nevada, Las Vegas

Thesis Title:

Conformal Mapping Improvement of the Boundary Element Method Solution for Underground Water Flow in a Domain with a Very Singular Boundary

Thesis Examination Committee:

Chairperson, Angel Muleshkov, Ph.D.

Committee Member, Zhonghai Ding, Ph.D.

Committee Member, Michelle Robinette Ph.D.

Graduate Faculty Representative, Stephen Lepp, Ph.D.